PROSPECTIVE MORTALITY TABLES: TAKING HETEROGENEITY INTO ACCOUNT

Julien TOMAS [α] * Frédéric PLANCHET [α] †

[α] *ISFA - Laboratoire SAF* ‡

Abstract

The present article illustrates an approach to construct prospective mortality tables for which the data available are composed by heterogeneous groups observed during different periods. Without explicit consideration of heterogeneity, it is necessary to reduce the period of observation at the intersection of the different populations observation periods. This reduction of the available history can arm the determination of the mortality trend and its extrapolation. We propose a model taking explicitly into account the heterogeneity, so as to preserve the entire history available for all populations. We use local kernel-weighted log-likelihood techniques to graduate the observed mortality. The extrapolation of the smoothed surface is performed by identifying the mortality components and their importance over time using singular values decomposition. Then time series methods are used to extrapolate the time-varying coefficients. We investigate the divergences in the mortality surfaces generated by a number of previously proposed models on three levels. These concern the proximity between the observations and the model, the regularity of the fit as well as the plausibility and consistency of the mortality trends.

Keywords. Heterogeneity, Prospective mortality table, Local likelihood, Singular values decomposition, Cox model, Generalized linear models, Relational models, Life insurance, Graduation, Extrapolation.

Résumé

Cet article illustre une approche concernant la construction d'une table de mortalité prospective pour laquelle les données disponibles sont constituées de groupes a priori hétérogènes et observés sur des périodes diffrentes. Sans prise en compte explicite de l'hétérogénéité, il est nécessaire de réduire la période d'observation à l'intersection des périodes d'observation des diffèrentes populations. Cette réduction de l'historique disponible s'avère pénalisant pour la détermination des tendances d'évolution de la mortalité et ainsi son extrapolation. Nous proposons un modèle intégrant explicitement la prise en compte de l'hétérogénéité, à partir du modèle de Cox, pour permettre de conserver l'ensemble de historique disponible pour toutes les populations. Nous utilisons des méthodes non-paramétriques de vraisemblance locale pour graduer la mortalité observée. L'extrapolation de la surface ajustée est obtenue en identifiant dans en premier temps les composantes de la mortalité et leur importance dans le temps par une décomposition en valeurs singulières. Des méthodes de séries temporelles sont employées pour extrapoler les paramètres variant dans le temps. Nous analysons les divergences observées entre les surfaces de mortalité générées sur trois niveaux. Ceux-ci concernent la proximité entre les observations et le modèle, la régularité de l'ajustement ainsi que la plausibilité et la cohérence des tendances d'évolution de la mortalité.

Mots-clés. Hétérogénéité, Table de mortalité prospective, Vraisemblance locale, Décomposition en valeurs singulières, Modèle de Cox, Modèles linéaires généralisés, Modèles relationnels, Risque de modèle, Assurance vie, Graduation, Extrapolation.

This work has been supported by the BNP Paribas Cardif Chair "Management de la modélisation" and the French Institut des Actuaires. The views expressed in this document are the authors own and do not necessarily reflect those endorsed by BNP Paribas Cardif and Institut des Actuaires.

*Contact: julien.tomas@univ-lyon.fr. All computer programs are available on request.

†Contact: frederic.planchet@univ-lyon1.fr.

‡Institut de Science Financière et d'Assurances - Université Claude Bernard Lyon 1 - 50 Avenue Tony Garnier - 69366 Lyon - France

Contents

1 Introduction

In this article, we present an approach to construct prospective mortality tables for which the data available are composed by heterogeneous groups observed during different periods. The approach is motivated by having the largest available history to determine the mortality trends.

It has been observed that the human mortality has globally declined over the 20th century. Life expectancy is greater than ever before and continues to improve rapidly, see Pitacco *et al.* (2009, Ch.3). These improvements affect the pricing and reserving in life insurance and constitute a challenge for actuaries and demographers in modeling the longevity.

In a pension plan, the longevity risk is transferred from the policyholder to the insurer. The latter has to evaluate his liability with appropriate mortality tables. It is in this context that since 1993 the French regulatory tables for annuities have been dynamic taking in account the increase of the life expectancy. Dynamic (or prospective) mortality tables allow to determine the remaining lifetime for a group, not according to the conditions of the moment, but given the future developments of living conditions.

However, applying exogenous tables to the group considered may result in under-provisioning the annuities, when the mortality of the group is lower than of the reference population.

With the international regulations *Solvency II* and *IFRS* insurers are required to evaluate their liabilities from realistic assumptions leading to an evaluation of the *best estimate*. In consequence, for pensions regimes and more generally due to the longevity risk, insurers have to build specific mortality tables, taking into account the expected evolution of the mortality of their insured population, see Planchet and Kamega (2013). It is in this context that we apply our approach to the construction of a reference mortality table from portfolios of several insurance companies. This reference could be used to adjust the mortality specifically to each insured portfolio and construct entity specific dynamic mortality tables.

We are in the situation where the data available are composed by heterogeneous groups observed during different periods. Without explicit consideration of heterogeneity, it is necessary to reduce the period of observation at the intersection of the different populations observation periods. This reduction of the available history can arm the determination of the mortality trend and its extrapolation. We propose a model taking explicitly into account the heterogeneity so as to preserve the entire history available for all populations. The innovative aspect lies in the articulation of a Cox model in a preliminary step and methods to graduate and extrapolate the mortality to construct a mortality table summarizing the mortality experience of all populations. We use local kernel-weighted log-likelihood techniques to graduate the observed mortality in a second step. The extrapolation of the smoothed surface is then performed by identifying the mortality components and their importance over time using singular values decomposition. The number of parameters is determined according their explicative power. Then time series methods are used to extrapolate the time-varying coefficients.

This article is organized as follows. Section 2 has still an introductory purpose. It specifies the notation and assumptions used in the following. Section 3 describes our approach to take explicitly into account the heterogeneity in constructing prospective mortality tables. Section 4 presents an application concerning the construction of a reference table from portfolios of various French insurance companies. Finally, some remarks in Section 5 conclude the paper.

2 Notation, assumption

2.1 Notation

We analyze the mortality as a function of both the attained age x and the calendar year t. The force of mortality at attained age x for the calendar year t, is denoted by $\varphi_x(t)$. We denote $D_{x,t}$ the number of deaths recorded at attained age x during calendar year t from an exposure-to-risk $E_{x,t}$ that measures the time during individuals are exposed to the risk of dying. It is the total time lived by these individuals during the period of observation. We suppose that we have data line by line originating from a portfolio. To each of the observations i, we associate the dummy variable δ_i indicating if the individual i dies or not,

$$\delta_i = \begin{cases} 1 & \text{if individual } i \text{ dies,} \\ 0 & \text{otherwise,} \end{cases}$$

for $i = 1, \ldots, L_{x,t}$. We define the time lived by individual i before $(x+1)th$ birthday by τ_i. We assume that we have at our disposal i.i.d. observations (δ_i, τ_i) for each of the $L_{x,t}$ individuals. Then,

$$\sum_{i=1}^{L_{x,t}} \tau_i = E_{x,t} \quad \text{and} \quad \sum_{i=1}^{L_{x,t}} \delta_i = D_{x,t}.$$

2.2 Piecewise constant forces of mortality

We assume that the age-specific forces of mortality are constant within bands of time, but allowed to vary from one band to the next, $\varphi_{x+\tau}(t+\xi) = \varphi_x(t)$ for $0 \leq \tau < 1$ and $0 \leq \xi < 1$.

We denote by $p_x(t)$ the probability that an individual aged x in calendar year t reaches age $x+1$, and by $q_x(t) = 1 - p_x(t)$ the corresponding probability of death. The expected remaining lifetime of an individual reaching age x during calendar year t is denoted by $e_x(t)$.
Under the assumption of piecewise constant forces of mortality, we have for integer age x and calendar year t,

$$p_x(t) = \exp\big(-\varphi_x(t)\big) \quad \text{and} \quad \varphi_x(t) = -\log\big(p_x(t)\big).$$

.

3 The approach

Our approach can be summarized as follows:

i. From a proportional hazard model, we describe how the risk of the populations changes over time. The resulting coefficients are used in the following step to weight the exposure to risk of each population.

ii. We smooth the surface using non-parametric local kernel-weighted log-likelihood to estimate $\varphi_x(t)$ for $x \in [x_1, x_n]$ and $t = 1, \ldots, m$.

iii. We decompose the smoothed surfaces via a basis function expansion using the following model:

$$\log \widehat{\varphi}_x(t) = \mu(x) + \sum_{k=1}^{K} \beta_{t,k}\, \phi_k(x) + \varepsilon_t(x) \text{ with } \varepsilon_t(x) \sim \text{Normal}\big(0, \upsilon(x)\big), \tag{1}$$

where $\mu(x)$ is the mean of $\log \widehat{\varphi}_x(t)$ across years and $\{\phi_k(x)\}$ is a set of orthonormal basis functions.

iv. ARIMA models are fitted to each of the coefficients $\{\beta_{t,k}\}$, $k = 1, \ldots, K$.

v. We extrapolate the coefficients $\{\beta_{t,k}\}$, $k = 1, \ldots, K$, for $t = m+1, \ldots, m+h$ using the fitted time series models.

vi. Finally, we use the resulting forecast coefficients with (1) to obtain forecasts of $\varphi_x(t)$, $t = m+1, \ldots, m+h$.

3.1 Taking into account heterogeneity

In step **i.**, we propose to describe from a proportional hazard model how the risk of the populations changes over time. Assuming the proportional hazards assumption holds then it is possible to estimate from a Cox model the relative risk without any consideration of the hazard function. For the population p, we have the model:

$$\varphi_x^p(t) = \alpha_p \, \varphi_x^0(t),$$

with $\varphi_x^0(t)$ the hazard function unknown and $\alpha_p = \exp(\boldsymbol{z}_p^T \theta_p)$. In our case, the parameter θ_p measures the influence of belonging to the population p on the intensity and $\boldsymbol{z}_p^T$ is the vector of covariates for the individual i, i.e. a dummy variable indicating if the individual belongs to the population p. The resulting coefficients are used in a following step to weight the exposure to risk of each population.

With the notation of Section 2.2 and under the assumption of a piecewise constant force of mortality, the likelihood becomes

$$\mathcal{L}\big(\varphi_x(t)\big) = \exp\big(-E_{x,t} \, \varphi_x(t)\big) \big(\varphi_x(t)\big)^{D_{x,t}}.$$

The associated log-likelihood is

$$\ell\big(\varphi_x(t)\big) = \log \mathcal{L}\big(\varphi_x(t)\big) = -E_{x,t} \, \varphi_x(t) + D_{x,t} \log \varphi_x(t).$$

Maximizing the log-likelihood $\ell\big(\varphi_x(t)\big)$ gives $\widehat{\varphi}_x(t) = D_{x,t}/E_{x,t}$ which coincides with the central death rates $\widehat{m}_x(t)$. Then it is apparent that the likelihood $\ell\big(\varphi_x(t)\big)$ is proportional to the Poisson likelihood based on

$$D_{x,t} \sim \mathcal{P}\big(E_{x,t} \, \varphi_x(t)\big). \tag{2}$$

Thus it is equivalent to work on the basis of the *true* likelihood or on the basis of the Poisson likelihood, as recalled in Delwarde and Denuit (2005). In consequence, under the assumption of constant forces of mortality between non-integer values of x and t, we consider (2) to take advantage of the Generalized Linear Models (GLMs) framework.

Hence, we supposed the following Poisson model for the number of deaths of the population p:

$$D_{x,t}^p \sim \mathcal{P}\left(E_{x,t}^p \, \varphi_x^p(t)\right),$$

Aggregating the populations, we obtain

$$\sum_p D_{x,t}^p \sim \mathcal{P}\left(\sum_p E_{x,t}^p \, \varphi_x^p(t)\right),$$

and,

$$\sum_p D_{x,t}^p \sim \mathcal{P}\left(\sum_p E_{x,t}^p \, \alpha_p \, \varphi_x^0(t)\right).$$

The observed exposure to risk is weighted by the coefficient α_p obtained from the Cox model at the preliminary step. Hence, we consider the following model,

$$D^{\circ}_{x,t} \sim \mathcal{P}\left(E^{\circ}_{x,t} \exp(f(x,t))\right),$$

where $D^{\circ}_{x,t} = \sum_p D^p_{x,t}$, $E^{\circ}_{x,t} = \sum_p E^p_{x,t}\,\alpha_p$ and $f(x,t)$ is an unknown smooth function.

3.2 Local likelihood smoothing methods

When the size of the group is sufficient, we can construct a prospective mortality table with the intention of identifying the behavior of the insured population that would differ from the regulatory tables or more generally from the national standard. However, in practice the size of the group may be limited and the past experience is observed over a short period.

As mentioned in Planchet and Lelieur (2007), two approaches can be proposed to smooth the crude data and project the future mortality using past observations. We distinguish

i. Endogenous approaches, which consist of exploiting the information contained in the crude forces of mortality to obtain a smooth surface representing the data correctly, and yield a *realistic* projection. In case of a small volume of data, these techniques could lead to biased estimations of the mortality trend.

ii. Models using an external reference mortality table (exogenous approaches) that present a solution to overcome the difficulties associated with having a small volume of data. The idea is to adjust a reference table to the experience of a given set of data.

Considering the limited volume of data available, our attention is focused on the second class of models even though a comparison with the first approach is presented.

This smoothing step **ii.** reduces some of the inherent randomness in the observed data. For this purpose we compare the following models described in Table 1.

			Estimation method	
Model	Formula	Ref. table	Local lik.	Min. dist.
M1	$D^{\circ}_{x,t} \sim \mathcal{P}\left(E^{\circ}_{x,t}\ \exp\big(f(x,t)\big)\right)$		M1	
M2	$D^{\circ}_{x,t} \sim \mathcal{P}\left(E^{\circ}_{x,t}\ \exp\big(f\big(\log\big(\varphi^{\text{ref}}_x(t)\big)\big)\big)\right)$	INSEE	M2.INSEE	
		TG05	M2.TG05	
M3	$D^{\circ}_{x,t} \sim \mathcal{P}\left(E^{\circ}_{x,t}\ \varphi^{\text{ref}}_x(t)\ \exp\big(f(x,t)\big)\right)$	INSEE	M3.INSEE	
		TG05	M3.TG05	
M4	$\text{logit}\ \varphi_x(t) = \alpha + \beta\ \text{logit}\ \varphi^{\text{ref}}_x(t) + \epsilon_{x,t}$	INSEE		M4.INSEE
	where $\varphi_x(t) = D^{\circ}_{x,t}/E^{\circ}_{x,t}$	TG05		M4.TG05

Table 1: Description of the models and estimation method used in the first step.

The functions $f(\cdot)$ are unspecified smooth functions of attained age x and calendar year t, and forces of mortality according to a reference table $\varphi^{\text{ref}}_x(t)$.

With the terminology mentioned previously, Model M1 is an endogenous non-parametric approach. Model M2 is an exogenous non-parametric relational model. Model M3 is a mixture of endogenous and exogenous approaches including the expected number of deaths $E^{\circ}_{x,t}$ $\varphi^{\text{ref}}_x(t)$ according to an external reference table. Finally, model M5 is a semi-parametric brass-type relational model. This model implies that the differences between the observed mortality and the reference can be represented linearly with two parameters. The parameter α is an indicator of mortality affecting all ages identically while the parameter β modifies this effect with age. The estimation is done by minimizing a weighted distance between the estimated and observed forces of mortality. Moreover, M4 has the advantage of integrated estimation and forecasting, as the parameters α and β are constant.
The models M1, M2 and M3 are estimated by non-parametric methods. We considered local kernel-weighted log-likelihood methods to estimate the smooth functions $f(x,t)$ and $f\big(\log\big(\varphi^{\text{ref}}_x(t)\big)\big)$ for $x \in [x_1, x_n]$ and $t = 1, \ldots, m$. Statistical aspects of local likelihood techniques have been discussed extensively in Loader (1996), Fan *et al.* (1998), Loader (1999) and Tomas (2013).
These methods have been used in a mortality context by Delwarde *et al.* (2004), Debón *et al.* (2006), Tomas (2011) to graduate life tables with attained age. More recently, Tomas and Planchet (2013) have covered smoothing in two dimension and introduced adaptive parameters choice with an application to long-term care insurance. Local likelihood techniques have the ability to model relatively well the mortality patterns even in presence of complex structures and avoid to rely on experts opinion.
The extrapolation, for $t = m+1, \ldots, m+h$, relies only on the information contained in the smoothed surface. It is performed by identifying the mortality components and their importance over time using singular values decomposition. The number of parameters is determined according their explicative power. Then time series methods are used to extrapolate the time-varying coefficients.

We consider two external prospective tables for the first step of our approach as references for the exogenous relational models. One is the national demographic projections for the French population over the period 2007-2060, provided by the French National Office for Statistics, INSEE, Blanpain and Chardon (2010). These projections are based on assumptions concerning fertility, mortality and migrations. We choose the baseline scenario among a total of 27 scenarios. The baseline scenario is based on the assumption that until 2060, the total fertility rate is remaining at a very high level (1.95). The decrease in gender-specific and age-specific mortality rates is greater for men over 85 years old. The baseline assumption on migration consists in projecting a constant annual net-migration balance of $100,000$ inhabitants. We complete this table by adding the years 1996-2006 from a previous INSEE table. The extrapolated part of the table, i.e. 2011-2060, being regular, we smoothed the forces of mortality of the completed table using local kernel weighted log-likelihood to remove the erratic pattern of the years 1996-2010.
The second external reference table, denoted TG05, is a market table built for the entire French market provided by the French Institute of Actuaries, Planchet (2006). Originally, the table is generational and covers the period 1900-2005. We rewrite it as to obtain a prospective table covering the period 1996-2035. It is worth to mention that this table was constructing using mortality trends originating from the INSEE table where a prudence has been added. As a consequence, this table is not fully faithful to the data but incorporates prudence in an arbitrary manner.

3.3 Singular values decomposition

Lee and Carter (1992) or its variants are now the dominant methods of mortality forecasting in actuarial sciences. The Lee-Carter method has a number of advantages, among them simplicity. The method involves using the first principal component of the log-mortality matrix. In contrast to parametric approaches which specify the functional form of the age pattern of mortality in advance, principal components approaches estimate the age pattern from the data.

Improvements to the Lee-Carter estimation basis have been proposed. A Poisson log-likelihood approach has been developed in Brouhns *et al.* (2002b), Brouhns *et al.* (2002a) and Renshaw and Haberman (2003) to remedy to some of the drawbacks of the Lee-Carter approach, such as for instance the assumed homoskedasticity of the errors. Cosette *et al.* (2007) use a binomial maximum likelihood, and a negative binomial version of the Lee-Carter model has been developed by Delwarde *et al.* (2007) to take into account the over-dispersion phenomenon.

In the following, we use singular values decomposition and fit time series models to each component coefficient to obtain forecasts of the forces of mortality. We prefer smoothing the observed data first rather than smoothing the component directly to place relevant constraints on the smoothing more easily. The decomposition using an orthonormal basis (step **iii.**) is obtained via principal components analysis.

We want to find a set of K orthonormal functions $\phi_k(x)$ so that the expansion of each curve in terms of the basis functions approximates the curve as closely as possible. For a given K, the optimal orthonormal basis functions $\{\phi_k(x)\}$ minimize the mean integrated squared error

$$\text{MISE} = \frac{1}{n}\sum_{t=1}^{m}\int \varepsilon_t^2(x)\,dx$$

This basis set provides informative interpretation and coefficients $\{\beta_{t,k}\}$ that are uncorrelated, simplifying the forecasting method as multivariate time series models are not required.

In expression 1, the parameter μ_x is estimated as the mean of $\log\widehat{\varphi}_x(t)$. Then we estimate $\{\beta_{t,k}\}$ and $\{\phi_k(x)\}$ using a singular values decomposition. We compute the matrix $\boldsymbol{Z}$ of dimension $n\times m$ with element (x,t) noted $z_{x,t}$ given by $z_{x,t}=\log\widehat{\varphi}_x(t)-\widehat{\mu}_x$. We centered the $\log\widehat{\varphi}_x(t)$ according their temporal mean.

In the following, we approximate the matrix $\boldsymbol{Z}$ such as

$$\boldsymbol{Z}\approx\sum_{k=1}^{K}\beta_{t,k}\;\phi_k(x). \tag{3}$$

As in Delwarde and Denuit (2005), this problem is tackled by singular values decomposition of $\boldsymbol{Z}$.

Let $\boldsymbol{u}_k$ the kth eigen vector of the squared matrix $\boldsymbol{Z}^T\boldsymbol{Z}$ of dimension $m\times m$ and λ_k the corresponding eigen value. Thus,

$$\boldsymbol{Z}^T\boldsymbol{Z}\,\boldsymbol{u}_k=\lambda_k\boldsymbol{u}_k \quad\text{and}\quad \boldsymbol{u}_k^T\,\boldsymbol{u}_k=1.$$

If we multiply both sides of the previous expression by $\boldsymbol{Z}$, we obtain $\big(\boldsymbol{Z}\,\boldsymbol{Z}^T\big)\,\boldsymbol{Z}\,\boldsymbol{u}_k=\lambda_k\big(\boldsymbol{Z}\,\boldsymbol{u}_k\big)$.
In consequence, for every eigen vector $\boldsymbol{u}_k$ of $\boldsymbol{Z}^T\boldsymbol{Z}$ associated to the eigen value λ_k corresponds an eigen vector $\boldsymbol{Z}\,\boldsymbol{u}_k$ of $\boldsymbol{Z}\boldsymbol{Z}^T$ associated to the same eigen value λ_k. Hence, all the eigen values of $\boldsymbol{Z}^T\boldsymbol{Z}$ and $\boldsymbol{Z}\,\boldsymbol{Z}^T$ are equal.
Thus, with $\boldsymbol{v}_k$ the kth eigen vector of the squared matrix $\boldsymbol{Z}\boldsymbol{Z}^T$ of dimension $n\times n$ associated to the eigen value λ_k, we have, for $\lambda_k\neq 0$,

$$\begin{aligned}\boldsymbol{v}_k&=\frac{1}{\sqrt{\lambda_k}}\boldsymbol{Z}\,\boldsymbol{u}_k \\ \text{and}\quad \boldsymbol{u}_k&=\frac{1}{\sqrt{\lambda_k}}\boldsymbol{Z}^T\,\boldsymbol{u}_k.\end{aligned} \tag{4}$$

Starting from expression (4), we have the relation $\boldsymbol{Z}\,\boldsymbol{u}_k = \boldsymbol{v}_k\,\sqrt{\lambda_k}$, from which we multiply the two sides by $\boldsymbol{u}_k^T$ before summing over the all eigen values of $\boldsymbol{Z}^T\boldsymbol{Z}$,

$$\boldsymbol{Z}\left(\sum_k \boldsymbol{u}_k\boldsymbol{u}_k^T\right) = \sum_k \sqrt{\lambda_k}\boldsymbol{v}_k\,\boldsymbol{u}_k^T.$$

As the eigen vectors $\boldsymbol{u}_k$ are orthogonal and of norm 1, $\sum_k \boldsymbol{u}_k\boldsymbol{u}_k^T$ corresponds to the identity matrix, which leads to the following decompsition of the matrix $\boldsymbol{Z}$:

$$\boldsymbol{Z} = \sum_k \sqrt{\lambda_k}\boldsymbol{v}_k\,\boldsymbol{u}_k^T.$$

The last expression is the singular values decomposition. Finally, confronting expressions (3) and (4), we obtain

$$\widehat{\phi}_k(x) = \frac{\boldsymbol{v}_k}{\sum_i v_{k,i}} \quad \text{and} \quad \widehat{\beta}_{k,t} = \lambda_k\left(\sum_i v_{k,i}\boldsymbol{u}_k\right), \quad \text{assuming} \quad \sum_i v_{k,i} \neq 0.$$

The number K of basis functions depends on many considerations. It depends on the number of discrete points m in the original data, whether some level of smoothing is imposed by using $K < m$, on the efficiency of the basis functions in reproducing the behavior of the original functions, and so on. Here, we use the percentage of variance explained, i.e. $\lambda_k / \sum_k \lambda_k$, to measure the quality of the approximation (4) obtained by the kth component and select K accordingly.

3.4 Extrapolation of the time-varying coefficients

Stochastic methods of mortality forecasting have received considerable attention, see Booth (2006) and Booth and Tickle (2008) for recent reviews. The most widely used are those involving some forms of extrapolation often using time series methods. Extrapolative methods assume that future trends will essentially be a continuation of the past. In mortality forecasting, this is usually a reasonable assumption because of historical regularities as It is generally accepted that the demographic phenomenon of inertia is sufficient for extrapolation of past trends.

The estimated $\beta_{t,k}$'s can be extrapolated using Box-Jenkins time series methods. We need to forecast $\beta_{t,k}$ for $k = 1, \ldots, K$ and $t = m+1, \ldots, m+h$. For $K > 1$ this is a multivariate time series problem. However, due to the way the basis functions $\phi_k(x)$ have been chosen, the coefficients $\widehat{\beta}_{t,k}$ and $\widehat{\beta}_{t,l}$ are uncorrelated for $k \neq l$. As a consequence, univariate time series methods are adequate for forecasting each series $\{\widehat{\beta}_{t,k}\}$. It is expressed through the development of an ARIMA (p,d,q) model where p, d, and q are integers, greater than or equal to zero and refer to the order of the autoregressive, integrated and moving average parts of the model. Given the time series $\{\widehat{\beta}_{t,k}\}$, where t is an integer index, an ARIMA (p,d,q) model is described by

$$(1-B)^d\,\phi(B)\,\widehat{\beta}_{t,k} = \theta(B)\,Z_t, \quad \text{and} \quad \{Z_t\} \sim \text{White Noise } (\sigma^2), \tag{5}$$

where B is the backshift operator, $B\,\widehat{\beta}_{t,k} = \widehat{\beta}_{t-1,k}$, expressing the length of the previous data that the model uses to provide the forecasts, and $\phi()$ and $\theta()$ are polynomials of degrees p and q respectively. We consider a full range of ARIMA (p, d, q) models with $d = 0, 1, 2$ and $p, q = 0, 1, 2, 3, 4$ as candidates for the period effects. The Bayes information criterion (BIC) is calculated for each ARIMA model and, on the basis of this information, the parameters p, d and q are selected. We refer to Delwarde and Denuit (2003) for an exhaustive application to the Lee-Carter model.

Then, extrapolated forces of mortality are derived using estimated $\mu(x)$ and $\mathbf{\Phi}$, the set of the basis functions, and extrapolated $\{\beta_{t,k}\}$. Time series models have the advantage of being stochastic, enabling the calculation of the probabilistic prediction intervals for the forecast value.
Conditioning on the observed data $\mathcal{J} = \{\varphi_t(x_i);\ t = 1, \ldots, m\ ; i = 1, \ldots, n\}$ and on the set of the basis function $\mathbf{\Phi}$, we deduce h-step ahead forecasts of $\varphi_{m+h}(x)$

$$\widehat{\varphi}_{m,h}(x) = \mathbb{E}\big[\varphi_{m+h}(x)|\mathcal{J}, \mathbf{\Phi}\big] = \widehat{\mu}(x) + \sum_{k=1}^{K} \tilde{\beta}_{m,h,k}\ \widehat{\phi}_k(x),$$

where $\tilde{\beta}_{m,h,k}$ denotes the h-step ahead forecasts of $\beta_{m+h,k}$ using the estimated series $\widehat{\beta}_{1,k}, \ldots, \widehat{\beta}_{m,k}$.

3.5 Completion

Finally, we would need to close the tables. Actuaries and demographers have developed various techniques for the completion of the tables at high ages, see among others Denuit and Quashie (2005) for a review. In this article, we use a simple and efficient method proposed by Denuit and Goderniaux (2005). This method relies on the adjusted one year probabilities of death and introduces two constraints about the completion of the mortality table. It consists to adjust, by ordinary least squares, the following log-quadratic model:

$$\log\ \widehat{q}_x(t) = a_t + b_t\ x + c_t\ x^2 + \epsilon_x(t), \quad \text{with} \quad \widehat{q}_x(t) = 1 - \exp\big(1 - \widehat{\varphi}_x(t)\big), \tag{6}$$

where $\epsilon_x(t) \sim$ iid Normal$(0, \sigma^2)$, separately for each calendar year t at attained ages x^*. Two restrictives conditions are imposed:

i. Firstly, a completion constraint,

$$q_{130}(t) = 1\ , \quad \text{for all } t.$$

Even though human lifetime does not seem to approach any fixed limit imposed by biological factors or other, it seems reasonable to accept the hypothesis that the age limit of end of life 130 will not be exceeded.

ii. Secondly, an inflexion constraint,

$$\frac{\partial}{\partial x} q_x(t)|_{x=130} = 0\ , \quad \text{for all } t.$$

These constraints impose concavity at older ages in addition to the existence of a tangent at the point $x = 130$. They lead to the following relation between the parameters a_t, b_t and c_t for each calendar year t:

$$a_t + b_t\ x + c_t\ x^2 = c_t\ (130 - x)^2,$$

for $x = x_t^*, x_t^* + 1, \ldots$. The parameters c_t are estimated from the series $\{\widehat{q}_x(t), x = x_t^*, x_t^* + 1, \ldots\}$ of calendar year t with equation (6) and the constraints imposed.

4 Construction of a dynamic reference table

4.1 The data

Data are originating from 8 portfolios of various French insurance companies, denoted P1, P2, ..., P8. Tables 2 and 3 display the observed statistics of the male and female data respectively.

					Period of observation	
Portfolios	Mean Age In	Mean Age Out	Mean Expo	Mean Age at death	Beginning	End
P1	40.92	49.10	8.18	60.58	01/01/1996	31/12/2010
P2	41.54	45.36	3.818	52.30	01/01/2005	31/12/2010
P3	44.43	46.69	2.26	77.04	01/07/2004	30/06/2007
P4	51.43	61.74	10.31	77.92	01/01/1996	31/12/2007
P5	41.57	46.60	5.03	55.83	01/01/2003	31/12/2009
P6	48.06	55.20	7.14	73.87	01/01/1996	31/12/2009
P7	48.81	52.79	3.97	73.51	01/01/2006	31/12/2010
P8	46.44	55.10	3.66	62.15	01/01/2005	31/12/2009

Table 2: Statistiques observes par portefeuille, population masculine.

					Period of observation	
Portfolios	Mean Age In	Mean Age Out	Mean Expo	Mean Age at death	Beginning	End
P1	41.36	49.43	8.08	64.20	01/01/1996	31/12/2010
P2	40.29	44.05	3.76	50.60	01/01/2005	31/12/2010
P3	49.66	51.94	2.28	83.61	01/07/2004	30/06/2007
P4	55.79	65.94	10.15	84.80	01/01/1996	31/12/2007
P5	42.58	47.55	4.97	57.74	01/01/2003	31/12/2009
P6	50.71	57.73	7.03	79.60	01/01/1996	31/12/2009
P7	49.08	53.00	3.93	80.58	01/01/2006	31/12/2010
P8	47.50	51.13	3.63	64.88	01/01/2005	31/12/2009

Table 3: Statistiques observes par portefeuille, female population.

The tables illustrate that the structure of the heterogeneity is changing over time as the portfolios are not observed during the same period.

4.2 Adjusting the relative risk

The changes in the structure of the heterogeneity over time may impact the estimation of the mortality trends over the years. Ideally we should have stuck to the same structure of the heterogeneity. In the following, we use the proportional hazard Cox type model to describe how the risk of the populations changes over time. Tables 4 and 5 present the resulting coefficients for the male and female population. They are then used in a following step to weight the exposure of each portfolio to adjust their relative risk.

Portfolio	coef	exp(coef)	se(coef)	z	$\mathbb{P}[>\|z\|]$
P1	0.17040	1.18578	0.02361	7.217	$5.31e-13$
P2	−0.18497	0.83113	0.02586	−7.152	$8.56e-13$
P3	0.40821	1.50412	0.02077	19.654	$< 2e-16$
P4	0.30299	1.35391	0.02362	12.830	$< 2e-16$
P5	0.30886	1.36187	0.01556	19.848	$< 2e-16$
P6	0.05362	1.05508	0.01417	3.785	0.000154
P7	−0.14291	0.86683	0.01802	−7.930	$2.22e-15$

Table 4: Estimated coefficients of the Cox model, male population.

Portfolio	coef	exp(coef)	se(coef)	z	$\mathbb{P}[>\|z\|]$
P1	0.20104	1.22268	0.03512	5.724	$1.04e-08$
P2	−0.31841	0.72731	0.04313	−7.383	$1.55e-13$
P3	0.36181	1.43592	0.02335	15.495	$< 2e-16$
P4	0.30529	1.35702	0.02428	12.573	$< 2e-16$
P5	0.23416	1.26385	0.02237	10.470	$< 2e-16$
P6	0.15235	1.16457	0.01884	8.086	$6.66e-16$
P7	0.05308	1.05451	0.02264	2.344	0.0191

Table 5: Estimated coefficients of the Cox model, female population.

We aggregate the portfolios by attained age x and calendar year t and weight the exposure with the coefficients obtained from the Cox models. The age range is 30 - 90 and the observations cover the period 01/01/1996 - 31/12/2010, i.e. the union of the different periods of observation. Figure 5, in Appendix A, displays the observed statistics of the aggregated datasets weighted by the coefficients obtained from the Cox model for the male and female population.

4.3 Comparisons of the fits

We fitted the models presented in Table 1. Figure 6 in Appendix B displays the fits in the log scale for the 7 models over the years for several ages. It gives us the opportunity to visualize the similarities and differences between the smoothed surfaces obtained by the models.

We observe that the models have the following features in common. The overall level of mortality has been declining over time and these improvements have been greater at lower ages than at higher ages. However the models diverge in the level and speed of the improvement. For instance, models using the national population table originating from INSEE have a greater speed of improvement than models using the market table.

In the following section, these visual comparisons are supplemented by a range of quantitative diagnostics which will increase our confidence in some models and question the suitability of others for our purposes.

4.4 Tests and quantities to compare graduations

We now carry out a number of tests to assess the impact of model choice. These concerns the proximity between the observations and the model as well as the regularity of the fit. We apply the tests proposed by Forfar *et al.* (1988), Debón *et al.* (2006), Tomas and Planchet (2014a) and Tomas and Planchet (2014b). We have also obtained the values of the mean absolute percentage error $MAPE$ and R^2 used in Felipe *et al.* (2002). In addition, we use the SMR test proposed by Liddell (1984).

Table 6 presents the results. We evaluate the fit according its regularity and the overall deviation from the past mortality. A satisfying fit, characterized by an homogeneous repartition of positive and negative signs of the response residuals and a high number of runs, should not lead to a significant gap with the past mortality, or vice versa. Accordingly, We balance these two complementary aspects in validating the model.

The approaches display different results. For the both populations, model M1, having the highest degrees of freedom and being fully endogenous, has the capacity to reveal many features in the data. Therefore, it has the lowest χ^2 and deviance, lowest number of standardized residuals exceeding the thresholds 2 and 3.
Conversely, the exogenous semi-parametric models M4 lead to the highest deviance, χ^2 and $MAPE$, and lowest R^2. In addition, they have the highest relative difference between expected and observed number of deaths.
The non-parametric exogenous models M2, being more flexible, perform better than the semi-parametric models M4. With respect to the reference table used, models M2 have a lower deviance, lower number of standardized residuals exceeding the thresholds 2 and 3, lower χ^2 and $MAPE$, and higher R^2. Also, the expected and observed number of deaths are closer.

		Male population							Female population						
		M1	M2.INSEE	M2.TG05	M3.INSEE	M3.TG05	M4.INSEE	M4.TG05	M1	M2.INSEE	M2.TG05	M3.INSEE	M3.TG05	M4.INSEE	M4.TG05
Fitted DF		7.551	3.466	3.384	4.098	4.081	NA	NA	7.695	3.499	3.564	4.201	4.212	NA	NA
χ^2		1098.37	1208.35	1200.77	1241.53	1255.19	1399.63	1371.80	1051.54	1105.20	1185.67	1116.77	1183.380	1211.48	1273.43
R^2		0.9450	0.9400	0.9462	0.9435	0.9474	0.9084	0.9453	0.9603	0.9581	0.9588	0.9605	0.9610	0.9528	0.9604
$MAPE$ (%)		22.28	22.90	22.03	22.03	21.63	25.92	25.18	25.11	24.89	24.74	24.60	24.68	28.36	26.30
Deviance		1106.43	1201.26	1194.61	1203.69	1228.55	1455.01	1413.10	1098.83	1121.22	1169.51	1124.64	1172.19	1287.71	1278.97
Standardized residuals	> 2	54	60	62	64	65	74	76	50	55	67	58	66	67	77
	> 3	6	11	10	12	15	16	14	7	8	12	9	13	9	15
SMR test	SMR	0.9822	0.9964	0.9957	0.9987	1.0033	0.9785	0.9877	0.9723	0.9952	0.9936	0.9975	1.0006	0.9868	0.9975
	ξ^{SMR}	2.4644	1.7246	0.9056	.0.4364	0.8911	3.8855	2.0736	4.7136	0.8012	1.0681	.0.4203	0.1055	2.2149	0.4141
	p-value	0.0137	0.0846	0.3652	0.6626	0.3729	$1e-04$	0.0381	0	0.2115	0.1427	0.3371	0.4580	0.0134	0.3394
Wilcoxon test	W	229242	223326	216777	213025	216661	240606	226117	228644	209796	229904	222749	227949	215582	239687
	ξ^{W}	2.4644	1.7246	0.9056	.0.4364	0.8911	3.8855	2.0736	2.3896	0.0326	2.5472	.1.6524	2.3027	0.7561	3.7706
	p-value	0.0137	0.0846	0.3652	0.6626	0.3729	$1e-04$	0.0381	0.0169	0.9740	0.0109	0.0984	0.0213	0.4496	$2e-04$
Signs test	$+(-)$	430(485)	433(482)	440(475)	455(460)	464(451)	395(520)	495(520)	417(498)	453(462)	469(446)	470(445)	486(429)	415(500)	475(440)
	ξ^{SIG}	1.7852	1.5868	1.1240	0.1322	0.3967	4.0993	4.0993	2.6447	0.2645	0.7273	0.7934	1.8513	2.7770	1.1240
	p-value	0.0742	0.1126	0.2610	0.8948	0.6916	0	0	0.0082	0.7914	0.4670	0.4275	0.0641	0.0055	0.2610
Runs test	Nber of runs	440	434	438	436	410	390	388	438	442	422	444	418	388	390
	ξ^{RUN}	1.1185	1.5384	1.3138	1.4876	3.2030	4.0422	4.1771	1.1278	1.0887	2.3970	0.9373	2.5718	4.4411	4.4939
	p-value	0.2633	0.1240	0.1889	0.1369	0.0014	$1e-04$	0	0.2594	0.2763	0.0165	0.3486	0.0101	0	0

Table 6: Comparisons between the smoothing approaches.

The mixtures of endogenous and exogenous modeling M3 perform better than models M2. Models M3 have a better spread of the residuals between positive and negative signs, higher R^2, lower $MAPE$ and higher p-value for the SMR test.
We observe that, in general, models incorporating the national population table originating from INSEE produce graduations that are closer to the experience data obtained from the female population than models using the market table TG05 as reference. For the male population, the models using the market table TG05 seem more satisfactory.

The tests and quantities carried out in Table 6 show the strengths and weaknesses of each model to adjust the observed mortality. The choice between the models is only a matter of judgment and depends on the purpose for which the prospective mortality table would be used. It is up to potential users of the table to decide the weights they place on the different criteria.

4.5 Extrapolation of the smoothed surfaces and completed tables

Figures 7 and 8, in Appendix C, display the basis functions and associated coefficients using equation (1) for the models M1, M2 and M3. For our application, 15 sampling points are available per curve and actually for these data a value of K as small as 2 captures most of the interesting variation in the original data, Tables 7 and 8.

	M1	M2.INSEE	M2.TG05	M3.INSEE	M3.TG05
1*st* coef	99.60	99.93	99.90	99.86	99.79
2*nd* coef	0.38	0.03	0.08	0.06	0.18

Table 7: Percentage of the variance explained, male population.

	M1	M2.INSEE	M2.TG05	M3.INSEE	M3.TG05
1*st* coef	91.26	98.01	86.19	96.65	91.51
2*nd* coef	6.42	0.81	5.71	1.81	4.11

Table 8: Percentage of the variance explained, female population.

The average log-mortality at attained ages is similar for the models over time, Figures 7a and 7d. Figures 7b and 7d show the first basis function for all models. The first term accounts for at least 86 % of the variation in mortality. The coefficient, Figures 8a and 8c, indicates a fairly steady decline in mortality over time. The basis function $\phi_1(x)$ indicates that the decline has been faster for the young adults. However, for the non-parametric exogenous models using the market table TG05, the decrease has been greater for females aged $60-80$ than the young female adults.
The basis function $\phi_2(x)$, Figures 7c and 7f, is more complicated and we do not try to explicate it. The shape of associated coefficient Figures 8b and 8d is more irregular. Again we observed that the choice of the reference table leads to a different pattern of the basis functions and associated coefficients.

The time-varying coefficients are forecast using univariate time series methods. Table 9, in Appendix C, summarizes the ARIMA models, introduced in Section 3.4.

For each of the models M1, M2 and M3, we considered a full range of ARIMA(p,d,q) models with $d = 0, 1, 2$ and $p, q = 0, 1, 2, 3, 4$ as candidates for the period effects. The Bayes information criterion (BIC) was calculated for each ARIMA model and, on the basis of this information, the parameters p, d and q have been selected. Figures 8e, 8f, 8g and 8h display the resulting projections for models M1, M2 and M3 for $h = 28$, that is until year 2035. For clarity, the confidence intervals are omitted.
We notice that some coefficients $\tilde{\beta}_{m,h,2}$ in Figures 8e and 8g are rapidly constant. As a consequence, we could have performed a decomposition using the first principal component as in the original Lee-Carter method. However, it may not be the case for other datasets, as illustrated in Hyndman and Ullah (2007) and Hyndman and Booth (2008).

The use of several components is the main difference between this approach and the Lee-Carter method, which uses only the first component and also involves an adjustment. The extra principal components allow more accurate forecasting of age-specific forces of mortality, though in our application at least 86 % of the variation is explained by the first component.

The next step is to complete the tables. We apply the model proposed by Denuit and Goderniaux (2005) to probabilities of death. We adjust the quadratic constraint regression (6). The optimal starting age x^* is selected over the range $[75, 85]$ for each calendar year.

The R^2 and corresponding estimated regression parameters c_t for the male and female population are displayed in Figure 9, in Appendix D, for the seven models. As an illustration, Figure 1a presents the results for Model M1 below.

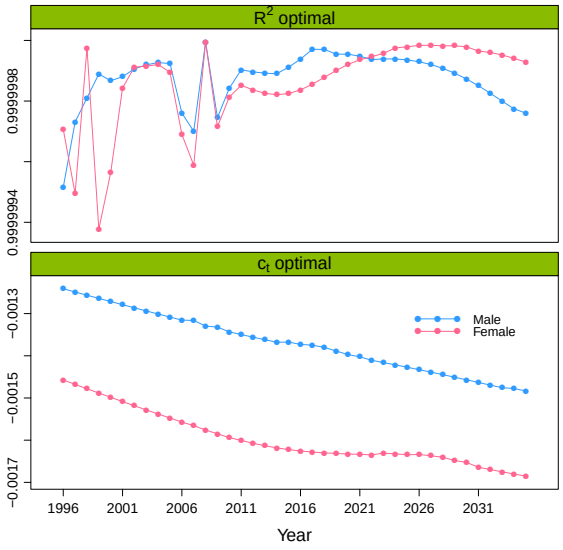

(a) R^2 et estimated c_t.

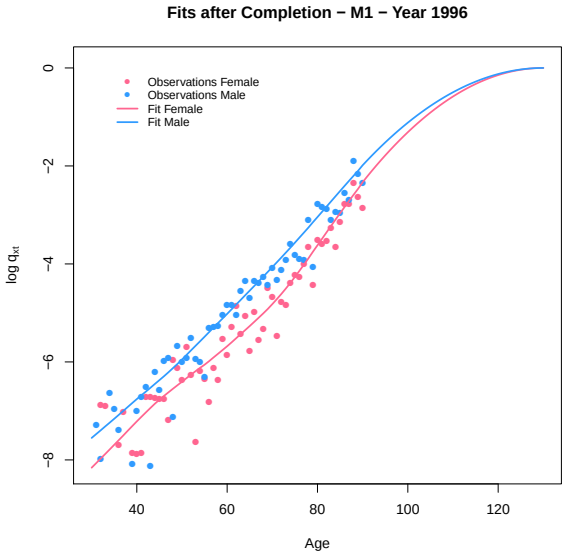

(b) Fits obtained after the completion for the calendar year 1996.

Figure 1: Estimated regression parameters and fits obtained by the completion method proposed by Denuit and Goderniaux (2005) for Model M1.

The models capture more than 99.99 % of the variance of the probabilities of death at high ages, Figure 1a top panel, for both populations. The regression parameters $\widehat{c}_t$ decrease relatively linearly with the calendar year, Figure 1a bottom panel.
This indicator represents the evolution of the mortality trends at high ages. We see that the mortality at high ages decreases and the speed of improvement is relatively similar for both populations for the exogenous models M2.TG05 and M4.TG05 using the market table as reference, Figures 9e and 9g. Models M2.INSEE, M3.INSEE and M4.INSEE using the national demographic projection as reference as well as M3.TG05 lead to a faster improvement of mortality for the female than the male population, Figures 9b, 9c, 9d and 9f. Only for the endogenous model M1 the female mortality tends to get closer to the male population over the years. We keep the original $\widetilde{q}_x(t)$ for ages below 85 years old for both populations, and replace the annual probabilities of death beyond this age by the values obtained from the quadratic regression. Results for the calendar year 1996 are presented, for both populations, in Figure 1b for Model M1 and in Figure 10, Appendix D, for the seven models.

Figure 11, in Appendix E, displays the fits of the probabilities of death in the log scale for the 7 models over the years for several ages. Figure 2, below, presents the results obtained for age 60. For clarity, the confidence intervals are omitted. The forecasts produced here are based on the two first decompositions. Compare to the original Lee-Carter method, the additional second component may serve to incorporate relatively recent changes in pattern. The use of smoothing prior to modeling results in forecast age patterns that are relatively smooth.

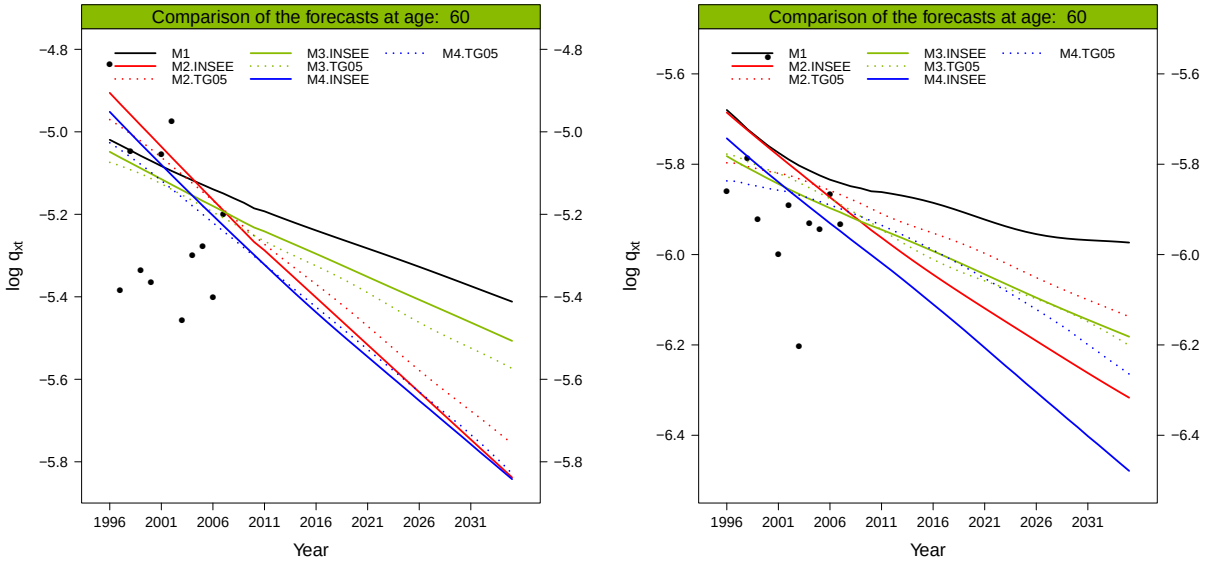

(a) Male population.

(b) Female population.

Figure 2: Comparisons of the fits and forecasts for age 60, log scale.

As visualized in Figure 6, the overall level of mortality is declining over time and these improvements are greater at lower ages than at higher ages. However the models diverge in the level and speed of the improvement. Exogenous models using the national demographic projection lead to a steeper decrease than models using the market table. Models having an endogenous component, M1 and M3, yield the slowest decline.

4.6 Plausibility and coherence of the forecasts

Validating the extrapolated future mortality is a much more difficult exercise than judging about the proximity about the observations and the model and a scientific statement about the future evolution of the mortality is impossible to make, Wilmoth (2011). Hence, one can only judge the reasonableness of the forecast and this has to be based on experts opinions such as biologists, physicians and demographers to yield the most objective assessment. Guidances have to question three factors regarding the consistency and the coherence. Those are the regularity and speed of improvement as well as the evolution between the male and female mortality when data are at our disposal.

About the regularity component, most authors suggest that the extrapolated future mortality should show a linear development. The human lifespan has been increasing for over a century as revealed by the records of extreme ages at death in Sweden for the last 130 years, see Wilmoth *et al.* (2000). From observations of national demographic statistics, Wilmoth (1998) has found that mortality has been falling gradually and maximum age at death has been rising steadily in the industrialized countries for more than 100 years. White (2002) finds a linear trend in life expectancy for all the high-income countries during the

second half of the 20th century. Oeppen and Vaupel (2002) argue that the process of mortality reductions should follow a stream of continuing progress and should not be seen as a disconnected sequence of unrepeatable revolutions.
About the speed of improvement, White (2002) also found that when a quadratic time trend was fitted to the standardized death rates, the coefficient on the squared term was significantly positive, indicating that the rate of improvement has been accelerating. Mortality improvements are the result of a complex process of advances in income, salubrity, nutrition, education, sanitation, and medicine, with the mix varying over age, period, cohort and place summarize Oeppen and Vaupel (2002). Thus, on the one hand the advance in life expectancy is a regular stream of continuous progress but on the other it is also a complex interaction between medical, social, economic factors, which sounds almost like a paradox for Bengtsson (2006). Possible increases in obesity and the possibility of pandemic diseases can question the continued long term trend of mortality improvements.
Finally, when we have at our disposal data of the male and female population exposed to the risk, we can assess the coherence of the forecasts by judging about the evolution of the mortality improvements of the two genders. It is well know that the mortality of males and females differs because of differences in their physiology, biology and behavior. After a large increase during the 19th and the 20th century, Meslé (2000) mentions that for two decades the gap in life expectancy between the two gender has been reducing in most industrialized countries. In France, where it was specially large, it stopped increasing in the early 1980s and decreased in the most recent years. For the author, it does not mean that female health situation is getting worse but it is related to an acceleration of progress for males. The difference will most probably reduce in the next years except if females would enjoy dramatic progression in old age mortality. For France and european countries (England and Wales, Sweden, Switzerland, Italy), taken as examples in Meslé (2000), the stabilization of the gap is mainly related to the decrease in cardiovascular mortality for men who benefit from the same progress but later than women. In the most recent years, the reduction of the gap is due to the trend reversal of male cancer mortality which is now decreasing, specially because of the reduction of lung cancer mortality, see Meslé (2000). Conversely, in Japan, the gap is still increasing specially for mortality from cancer and respiratory diseases.

Those considerations led Cairns *et al.* (2006) to propose the concept of *biological reasonableness* as an aid in assessing the forecasts. This concept is not based on hard scientific, biological or medical facts but should follow experts' opinions. It is rather subjective and asks the question where the data are originating from and based on this knowledge, what mixture of biological factors, medical advances and environmental changes would have to happen to cause this particular set of forecasts.

In the following, we evaluate singles indices summarizing the lifetime probability distribution for different cohorts at several ages such as the cohort life expectancies ${}_{\omega}e^{\nearrow}_{\widetilde{x}}$, median age at death $\text{Med}\left[{}_{\omega}T_{\widetilde{x}}\right]$ and the entropy $\text{H}\left[{}_{\omega}T_{\widetilde{x}}\right]$. Graphical diagnostics are also used to assess the consistency of the historical and forecasted periodic life expectancy ${}_{\omega}e^{\uparrow}_{x}(t)$, see Tomas and Planchet (2014a) and Tomas and Planchet (2014b). In addition, having at our disposal the male and female mortality, we can compare the trends of improvement and judge the plausibility of the common evolution of mortality of the two populations.

We obtain the survival function calculated from the completed tables. From the survival function, we derive a series of markers summarizing the lifetime probability distribution. We are interested in the survival distribution of cohorts aged $\widetilde{x} = 30$ to 90 years old in 1996 over 40 years. Hence, we are working along the diagonal of the Lexis diagram. Table 10, in Appendix F, presents the cohorts life expectancies, the median age at death and the entropy for both populations.

The exogenous models non-parametric M2 and semi-parametric M4 lead to the highest cohort life expectancies and median age at death until 70 years old. In consequence, the entropy is smaller and the deaths are more concentrated. At the opposite, the endogenous model M1, yields the smallest cohort life expectancies and median age at death and the deaths are most stretched.
We observe, once more, that the choice of the reference table affects the single indices summarizing the lifetime probability distribution. The exogenous models using the market table lead to a smaller cohort life expectancies and median age at death until 70 years old than models using the national demographic projection. Conversely, after 70 years old the relation is reversed.

Figure 12, in Appendix G, compares the trends in periodic life expectancies for the ages 35, 60 and 85 for the male and female population. As an illustration, Figure 3, below, presents the results obtained for age 60. We observe that the exogenous models lead to the highest predicted periodic life expectancies. Model M1, being fully endogenous yields the lowest. The mixture of endogenous et exogenous modeling models M3 follow adequately the observed trend.

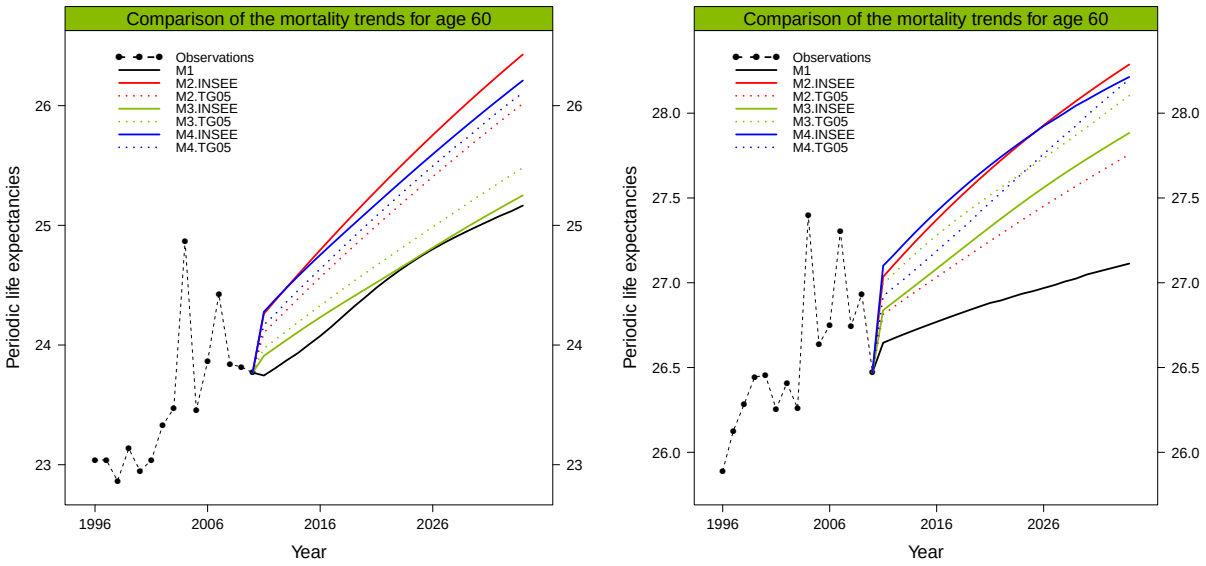

(a) Male population.

(b) Female population.

Figure 3: Comparison of the trends in periodic life expectancies for age 60.

In the following, we compare the mortality trends of the male and female population to judge the plausibility of the common improvement. Figure 13, in Appendix H, displays the ratio between the cohorts life expectancies over 5 years of the two genders. Figure 14, in Appendix H, presents the ratio between the fitted probabilities of death of the two genders. As an illustration, Figure 4, below, shows the results obtained for Model M1.

.

The cohorts life expectancies of the female population, Figure 4a, are 15 % larger than the male ones at 90 years old, 10 % at 80 and 5 % at 70 years old. The exogenous models M2 and M4 using the national demographic projection as well as models M3 lead to relatively similar mortality trends. The ratio tends to get closer to 1 for ages below 95 years old, and increases after 95 indicating that the female mortality is improving more rapidly than the male for the very high ages. Models M1 and the exogenous models

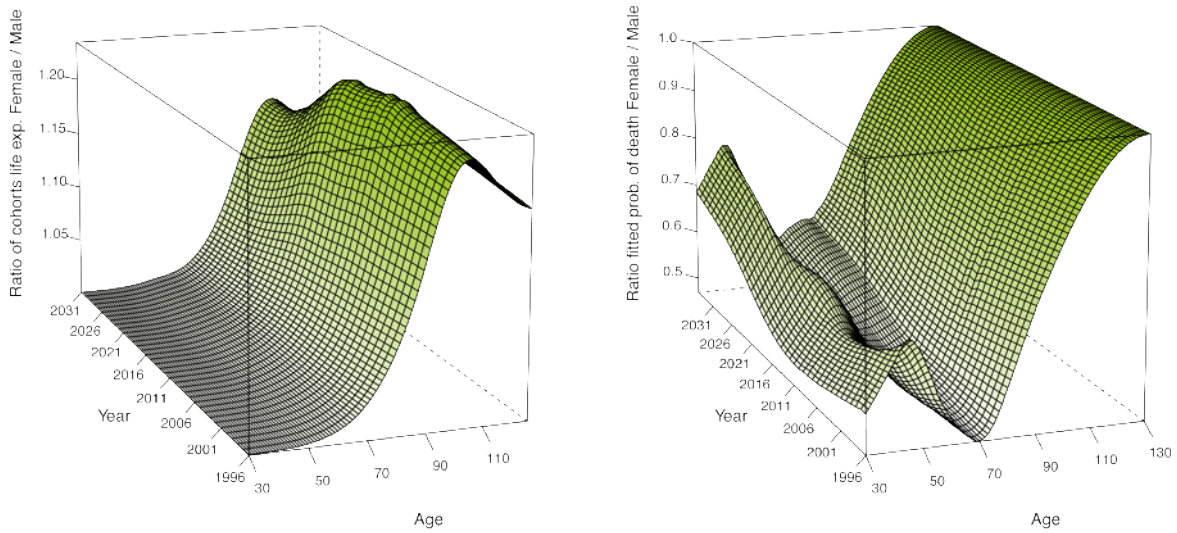

(a) Ratio of the cohort life expectancies over 5 years.

(b) Ratio of the fitted probabilities of death.

Figure 4: Comparison of the male and female mortality, female / male, model M1.

M2 and M4 using the market table as reference yield a faster improvement of the male mortality than the female for every ages, which seems to be coherent.
The ratio of the extrapolated probabilities of death, Figure 4b, shows clearly that the male mortality is improving more rapidly than female for the young adult until 65 years old. The exogenous models M2 and M4 lead to the fastest improvement. However, for those models using the market table as reference, the female mortality becomes even higher than the male one at the end of the forecast period. If we cannot think about any good reason why this might happen, then we must disqualify these models on the basis of *biological reasonableness*. The projections of models M3 seem reasonable, in accordance with the set of projections with the other models.

5 Summary and outlook

In this article, we presented a an approach to construct prospective mortality tables for which the data available are composed by heterogeneous groups observed during different periods. The approach has been motivated by having the largest available history to determine the mortality trends.

We proposed a model taking explicitly into account the heterogeneity so as to preserve the entire history available for all populations. We applied a proportional hazard Cox type model in a preliminary step to describe how the risk of the populations changes over time. These coefficients have been used at the following step to weight the exposure to risk. We have used local kernel-weighted log-likelihood techniques to graduate the observed mortality in the second step. The extrapolation of the smoothed surface has been performed by identifying the mortality components and their importance over time using singular values decomposition. The number of parameters have been determined according their explicative power. Then time series methods are used to extrapolate the time-varying coefficients.

We have applied our methodology to the construction of a reference mortality table from portfolios of several insurance companies. This reference could be used to adjust the mortality specifically to each insured portfolio and construct entity specific dynamic mortality tables by a Poisson generalized linear

model including the reference has covariate and allowing age and calendar year interactions or by a semi-parametric relational model.

We investigated the differences in the mortality surfaces generated by a number of proposed models. Actuaries should acknowledge the use of multiple models rather than pretend that it is sufficient to adjust the past mortality and make forecasts based on any single model. The investigation of the divergences between the models has been assessed on three levels. The two first levels evaluate the fit according its regularity and the overall deviation from the past mortality. A satisfying fit, characterized by an homogeneous repartition of positive and negative signs of the response residuals and un high number of runs, should not result in a significant gap with the past mortality, or vice versa. Accordingly, the two first levels of the validation balance these two complementary aspects. The third level covers the coherence and consistency of the mortality trends. We asked the question where the data are originating from and based on this knowledge and experts' opinions, what mixture of biological factors, medical advances and environmental changes would have to happen to cause this particular set of forecasts.

Acknowledgment

This research was supported by grants from BNP Paribas Cardif Chair *Management de la modélisation* and Institut des Actuaires.
In addition, we are also grateful to a referee for a careful reading of the manuscript and comments which led to an improved version of the paper.

References

Bengtsson, T. (2006). Linear increase in life expectancy: past and present. In T. Bengtsson, editor, *Perspectives on mortality forecasting. III: The linear rise in life expectancy: history and prospects*, volume 3, pages 83–99. Swedish Social Insurance Agency.

Blanpain, N. and Chardon, O. (2010). Projections de populations 2007-2060 pour la France métropolitaine: méthode et principaux résultats. Série des Documents de Travail de la direction des statistiques Démographiques et Sociales F1008, Institut National de la Statistique et des Études Économiques.

Booth, H. (2006). Demographic forecasting: 1980 to 2005 in review. *International Journal of Forecasting*, **22**(3), 547–581.

Booth, H. and Tickle, L. (2008). Mortality modelling and forecasting: a review of methods. *Anals of Actuarial Science*, **3**(1/2), 3–43.

Brouhns, N., Denuit, M., and Vermunt, J. K. (2002a). Measuring the longevity risk in mortality projections. *Bulletin of the Swiss Association of Actuaries*, **2**, 105–130.

Brouhns, N., Denuit, M., and Vermunt, J. K. (2002b). A poisson log-bilinear regression approach to the construction of projected lifetables. *Insurance: Mathematics & Economics*, **31**, 373–393.

Cairns, A. J. G., Blake, D., and Dowd, K. (2006). Pricing death: Frameworks for the valuation and securization of mortality risk. *ASTIN Bulletin*, **36**, 79–120.

Cosette, H., Delwarde, A., Denuit, M., Guillot, F., and Marceau, E. (2007). Pension plan valuation and dynamic mortality tables. *North American Actuarial Journal*, **11**(2), 1–34.

Debón, A., Montes, F., and Sala, R. (2006). A comparison of nonparametric methods in the graduation of mortality: Application to data from the Valencia region (Spain). *International statistical Review*, **74**(2), 215–233.

Delwarde, A. and Denuit, M. (2003). Importance de la période d'observation et des âges considérés dans la projection de la mortalité selon la méthode de Lee-Carter. *Belgian Actuarial Bulletin*, **3**(1), 1–21.

Delwarde, A. and Denuit, M. (2005). *Construction de tables de mortalité périodiques et prospectives*. Assurance Audit Actuariat. Economica.

Delwarde, A., Kachkhdze, D., Olie, L., and Denuit, M. (2004). Modèles linéaires et additifs généralisés, maximum de vraisemblance local et méthodes relationelles en assurance sur la vie. *Bulletin Français d'Actuariat*, **6**(12), 77–102.

Delwarde, A., Denuit, M., and Partrat, C. (2007). Negative binomial version of the Lee-Carter model for mortality forecasting. *Applied Stochastic Models in Buisiness and Industry*, **23**(5), 385–401.

Denuit, M. and Goderniaux, A. C. (2005). Closing and projecting life tables using log-linear models. *Bulletin of the Swiss Association of Bulletin of the Swiss Association of Actuaries*, (1), 29–48.

Denuit, M. and Quashie, A. (2005). Modèles d'extrapolation de la mortalité aux grands âges. *Institut des Sciences Actuarielles et Institut de Statistique Université Catholique de Louvain Working Paper*, pages 1–19.

Fan, J., Farmen, M., and Gijbels, I. (1998). Local maximum likelihood estimation and inference. *Journal of the Royal Statistical Society*, **60**(3), 591–608.

Felipe, A., Guillén, M., and Pérez-Marín, A. (2002). Recent mortality trends in the Spanish population. *British Actuarial Journal*, **8**(4), 757–786.

Forfar, D., McCutcheon, J., and Wilkie, A. (1988). On graduation by mathematical formula. *Journal of the Institute of Actuaries*, **115**(part I(459)), 643–652.

Hyndman, R. J. and Booth, H. (2008). Stochastic population forecasts using functional data models for mortality, fertility and migration. *International Journal of Forecasting*, **24**(3), 323–342.

Hyndman, R. J. and Ullah, M. (2007). Robust forecasting or mortality and fertility rates: A functional data approach. *Computational Statistics & Data Analysis*, **51**(10), 4942–4956.

Lee, R. D. and Carter, L. R. (1992). Modeling and forecasting U.S. mortality. *Journal of the American Statistical Association*, **87**(419), 659–671.

Liddell, F. D. K. (1984). Simple exact analysis of the standardised mortality ratio. *Journal of Epidemiology and Community Health*, **38**, 85–88.

Loader, C. R. (1996). Local likelihood density estimation. *The Annals of Statistics*, **24**(4), 1602–1618.

Loader, C. R. (1999). *Local Regression and Likelihood*. Statistics and Computing Series. New York: Springer Verlag.

Meslé, F. (2000). Ecart d'espérance de vie entre les sexes : les raisons du recul de l'avantage féminin. *Revue d'Épidémiologie et de Santé Publique*, **52**(4), 333–352.

Oeppen, J. and Vaupel, J. W. (2002). Broken limits to life expectancy. *Science*, **296**(5570), 1029–1031.

Pitacco, E., Denuit, M., Haberman, S., and Olivieri, A. (2009). *Modelling longevity dynamics for pensions and annuity business*. Oxford University Press.

Planchet, F. (2006). Tables de mortalité d'expérience pour les portefeuilles de rentiers (tables TGH05 et TGF05). Technical report, Institut des Actuaires.

Planchet, F. and Kamega, A. (2013). Construction de tables de mortalité prospectives sur un groupe restreint: Mesure du risque d'estimation. *Bulletin Français d'Actuariat*, **13**(25).

Planchet, F. and Lelieur, V. (2007). Utilisation des méthodes de Lee-Carter et log-Poisson pour l'ajustement de tables de mortalité dans le cas de petits échantillon. *Bulletin Français d'Actuariat*, **7**(14), 118–146.

Renshaw, A. E. and Haberman, S. (2003). Lee-Carter mortality forecasting with age-specific enhancement. *Insurance: Mathematics & Economics*, **33**(2), 255–272.

Tomas, J. (2011). A local likelihood approach to univariate graduation of mortality. *Bulletin Français d'Actuariat*, **11**(22), 105–153.

Tomas, J. (2013). *Quantifying biometric life insurance risks with non-parametric methods*. Ph.D. thesis, Amsterdam School of Economics Research Institute.

Tomas, J. and Planchet, F. (2013). Multidimensional smoothing by adaptive local kernel-weighted log-likelihood with application to long-term care insurance. *Insurance: Mathematics & Economics*, **52**(3), 573–589.

Tomas, J. and Planchet, F. (2014a). Constructing entity specific prospective mortality table: adjustment to a reference. *European Actuarial Journal*, pages 1–32. To appear.

Tomas, J. and Planchet, F. (2014b). Prospective mortality table and portfolio experience. In A. Charpentier, editor, *Computational Actuarial Science, with R*, The R Series, chapter 9. Chapman and Hall. To appear.

White, K. M. (2002). Longevity advances in high-income countries, 1955-96. *Population and Development Review*, **28**(1), 59–76.

Wilmoth, J. R. (1998). The future of human longevity: a demographer's perspective. *Science*, **280**(5362), 395–397.

Wilmoth, J. R. (2011). Increase of human longevity: past, present, and future. *The Japanese Journal of Population*, **9**(1), 155–161.

Wilmoth, J. R., Deegan, L. J., Lundström, H., and Horiuchi, S. (2000). Increase of maximum life-span in sweden, 1861-1999. *Science*, **289**(5488), 2366–2368.

Appendix

A The data

Figure 5 displays the observed statistics of the aggregated datasets weighted by the coefficients obtained from the Cox model for the male and female population.

B Comparisons of the fits

Figure 6 presents the fits in the log scale for the 7 models over the years for several ages.

C Extrapolation of the smoothed surfaces

Figures 7 and 8 display the basis functions and associated coefficients using equation (1) for the models M1, M2 and M3. Table 9 summarizes the ARIMA models, introduced in Section 3.4.

D Completion

Figure 9 presents the R^2 and corresponding estimated regression parameters c_t for the male and female population for the seven models. The fits obtained after the completion for the calendar year 1996 are displayed in Figure 10.

E Comparison of the fits and forecasts

Figure 11 displays the fits of the probabilities of death in the log scale for the 7 models over the years for several ages.

F Single indices summarizing the lifetime probability distribution

Table 10 presents the cohorts life expectancies, the median age at death and the entropy for both populations.

G Comparison of the trends in periodic life expectancies

Figure 12 compares the trends in periodic life expectancies for the ages 35, 60 and 85 for the male and female population.

H Comparison of the evolution of the male and female mortality

Figure 14 and 13 present the ratio between the cohorts life expectancies over 5 years and the ratio between the fitted probabilities of death of the two genders respectively.

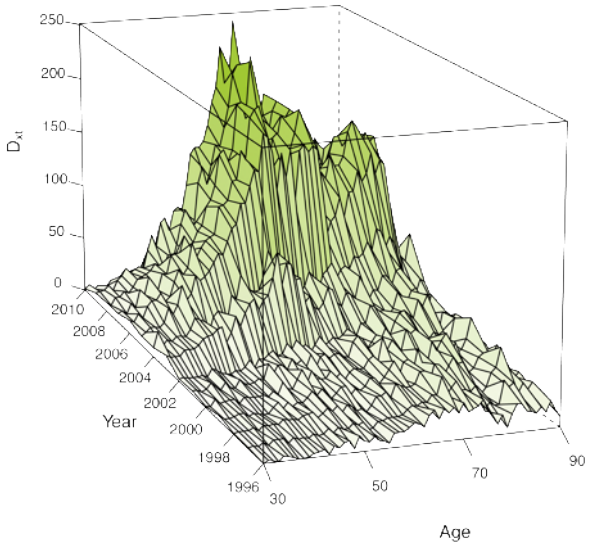

(a) $D^{\circ}_{x,t}$, male

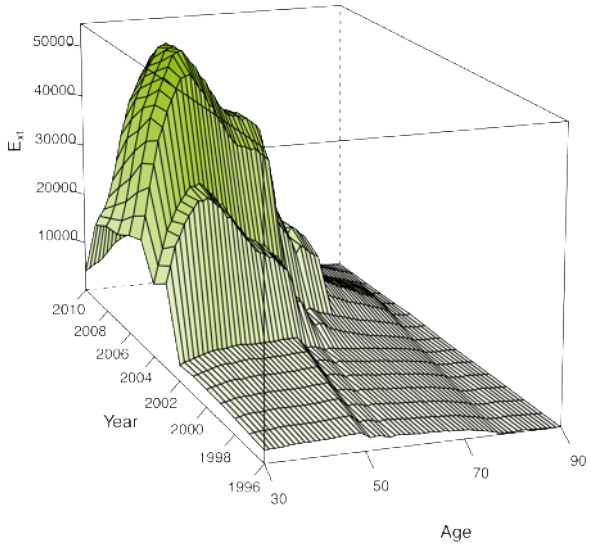

(b) $E^{\circ}_{x,t}$, male

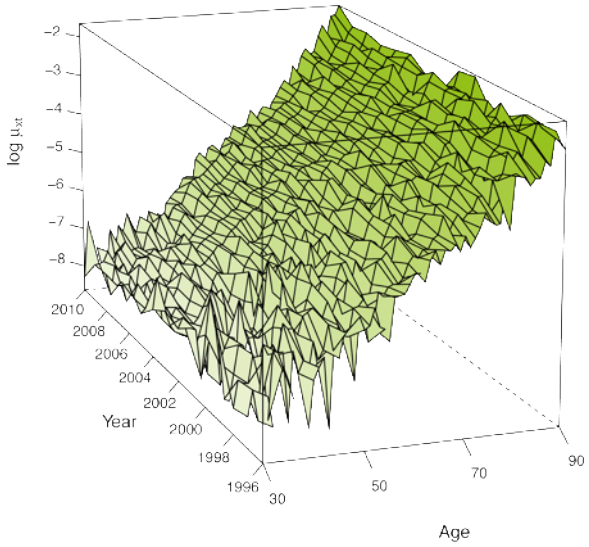

(c) $\log \varphi_x(t)$, male

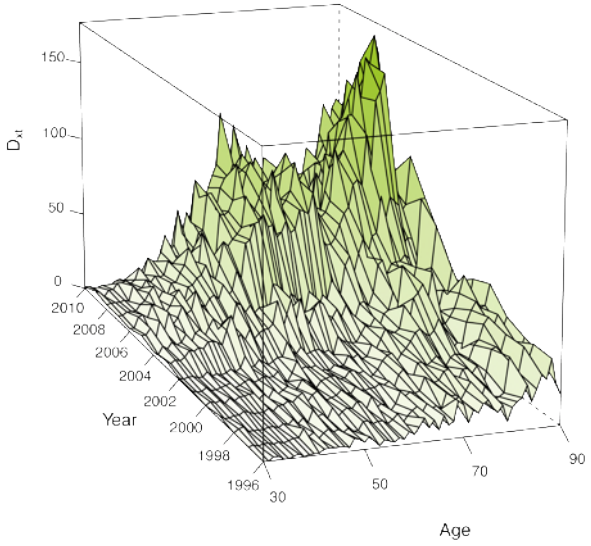

(d) $D^{\circ}_{x,t}$, female

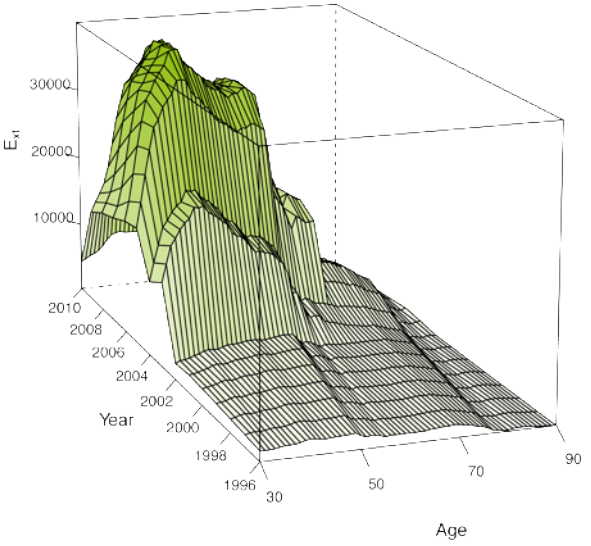

(e) $E^{\circ}_{x,t}$, female

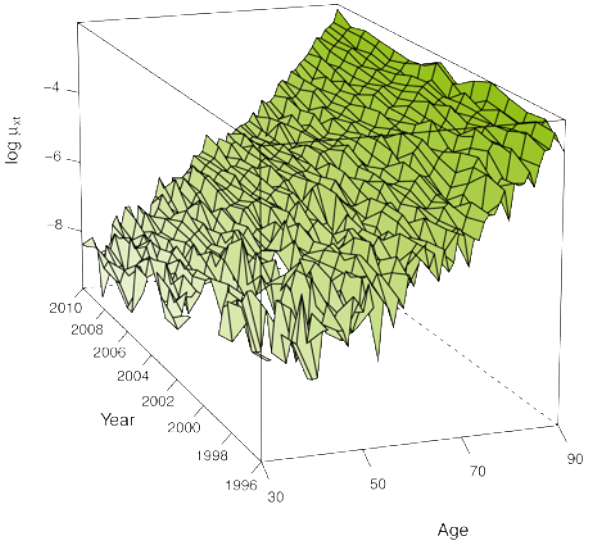

(f) $\log \varphi_x(t)$, female

Figure 5: Observed surfaces of the aggregated datasets.

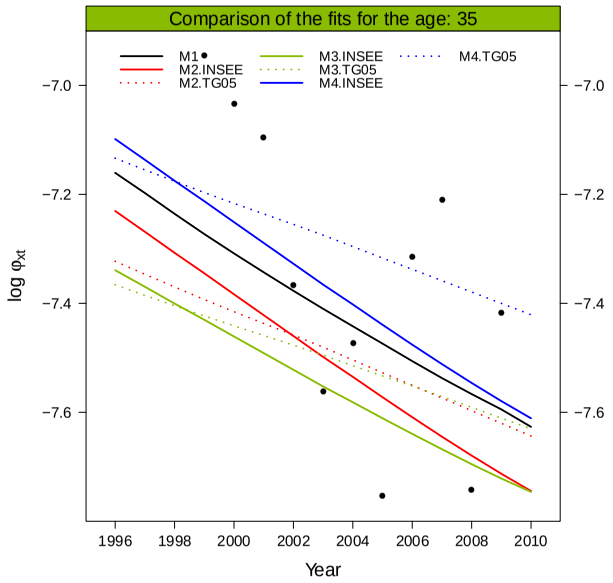

(a) Age 35, male

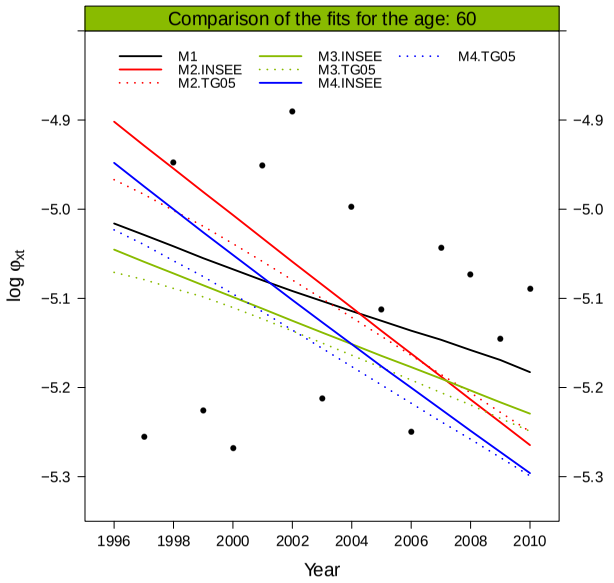

(b) Age 60, male

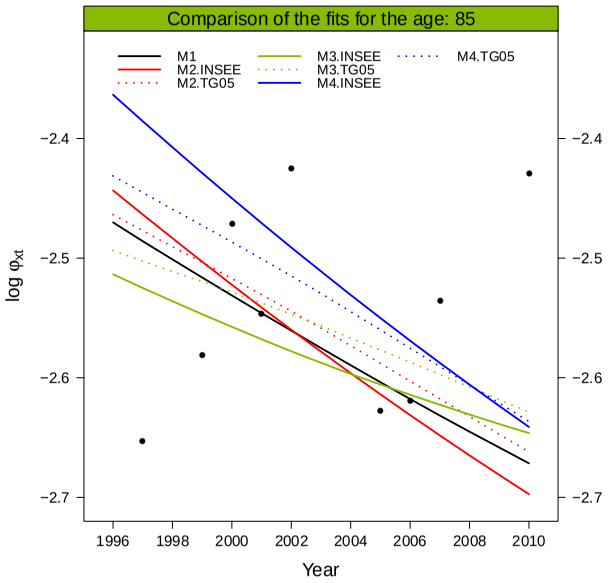

(c) Age 85, male

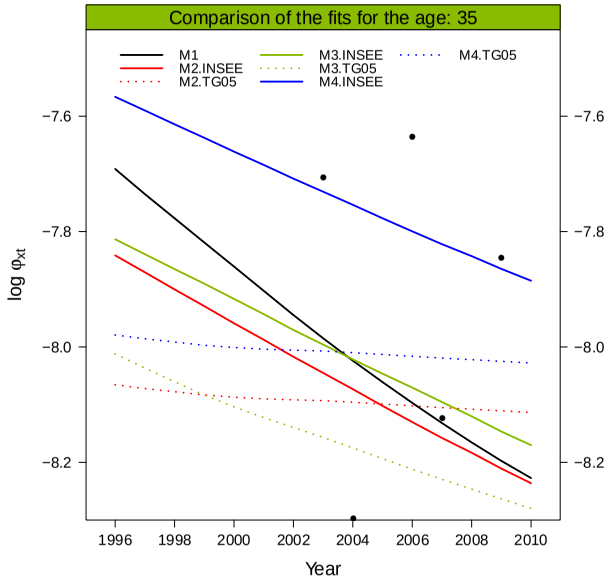

(d) Age 35, female

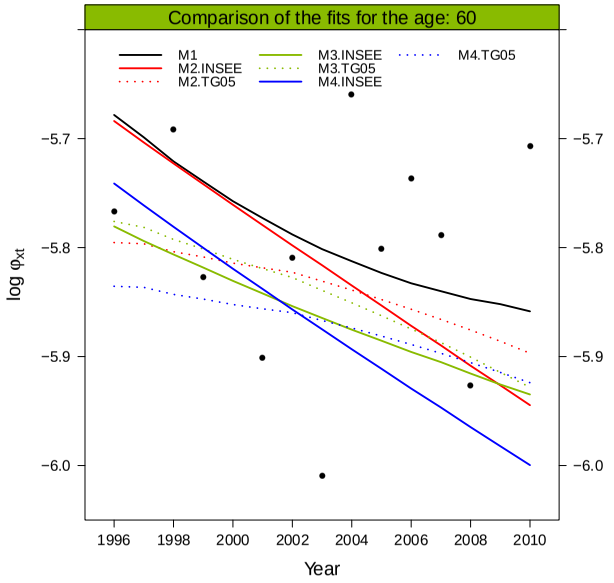

(e) Age 60, female

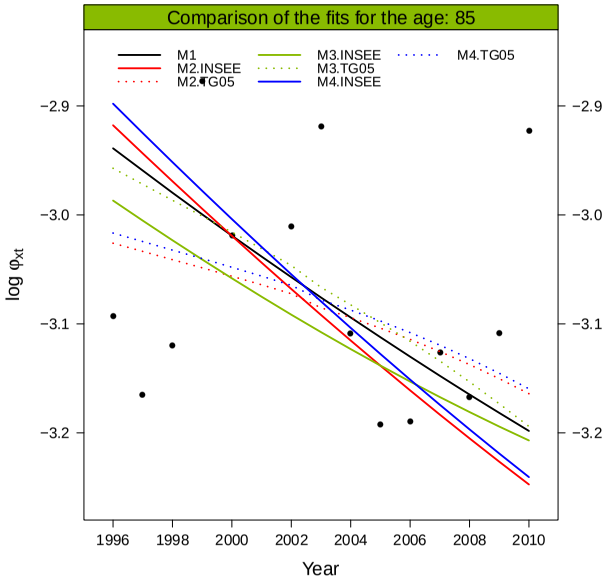

(f) Age 85, female

Figure 6: Comparisons of the Fits for several ages, log scale.

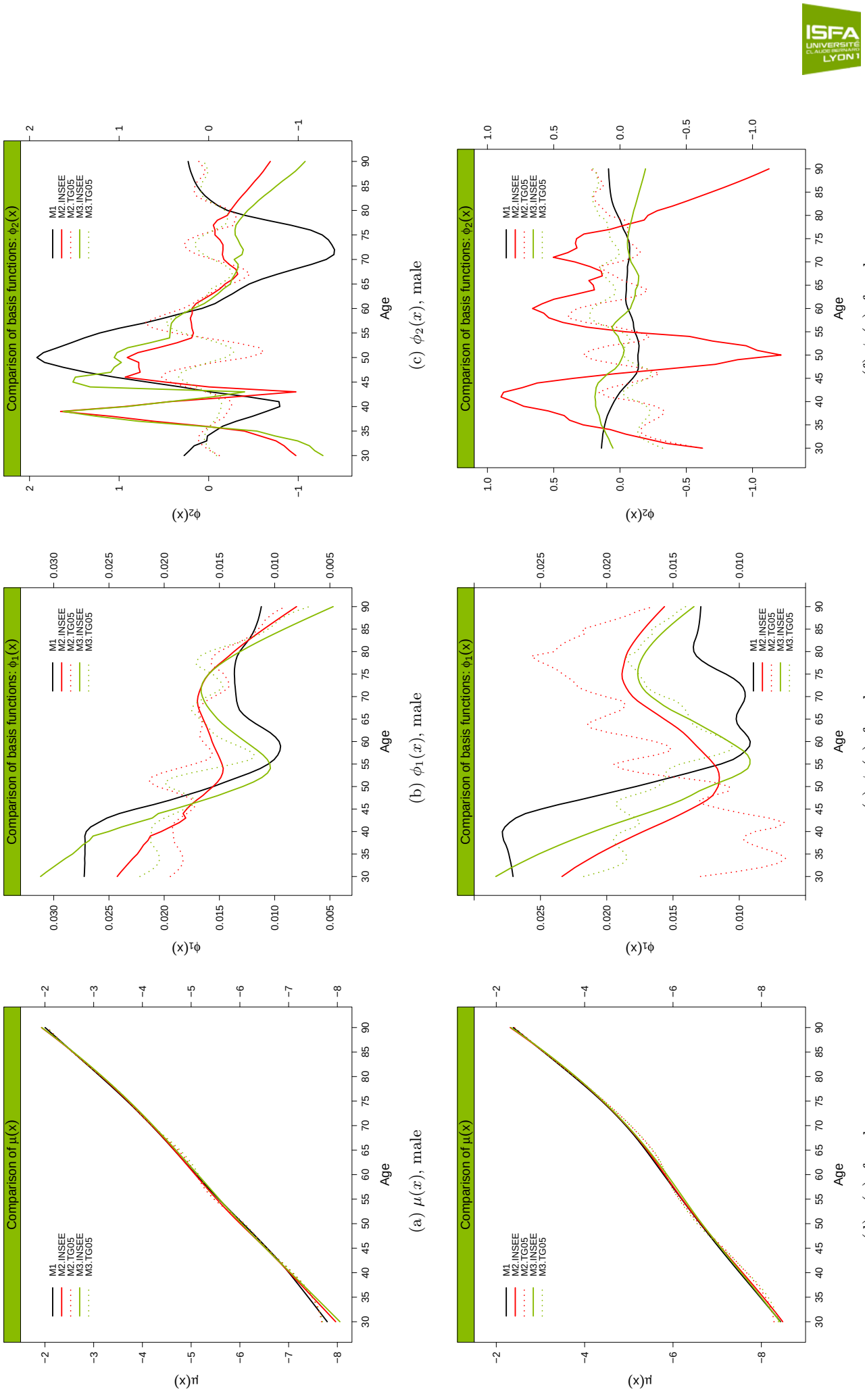

(a) $\mu(x)$, male (b) $\phi_1(x)$, male (c) $\phi_2(x)$, male

(d) $\mu(x)$, female (e) $\phi_1(x)$, female (f) $\phi_2(x)$, female

Figure 7: Basis functions with $K = 2$, for models M1, M2, and M3.

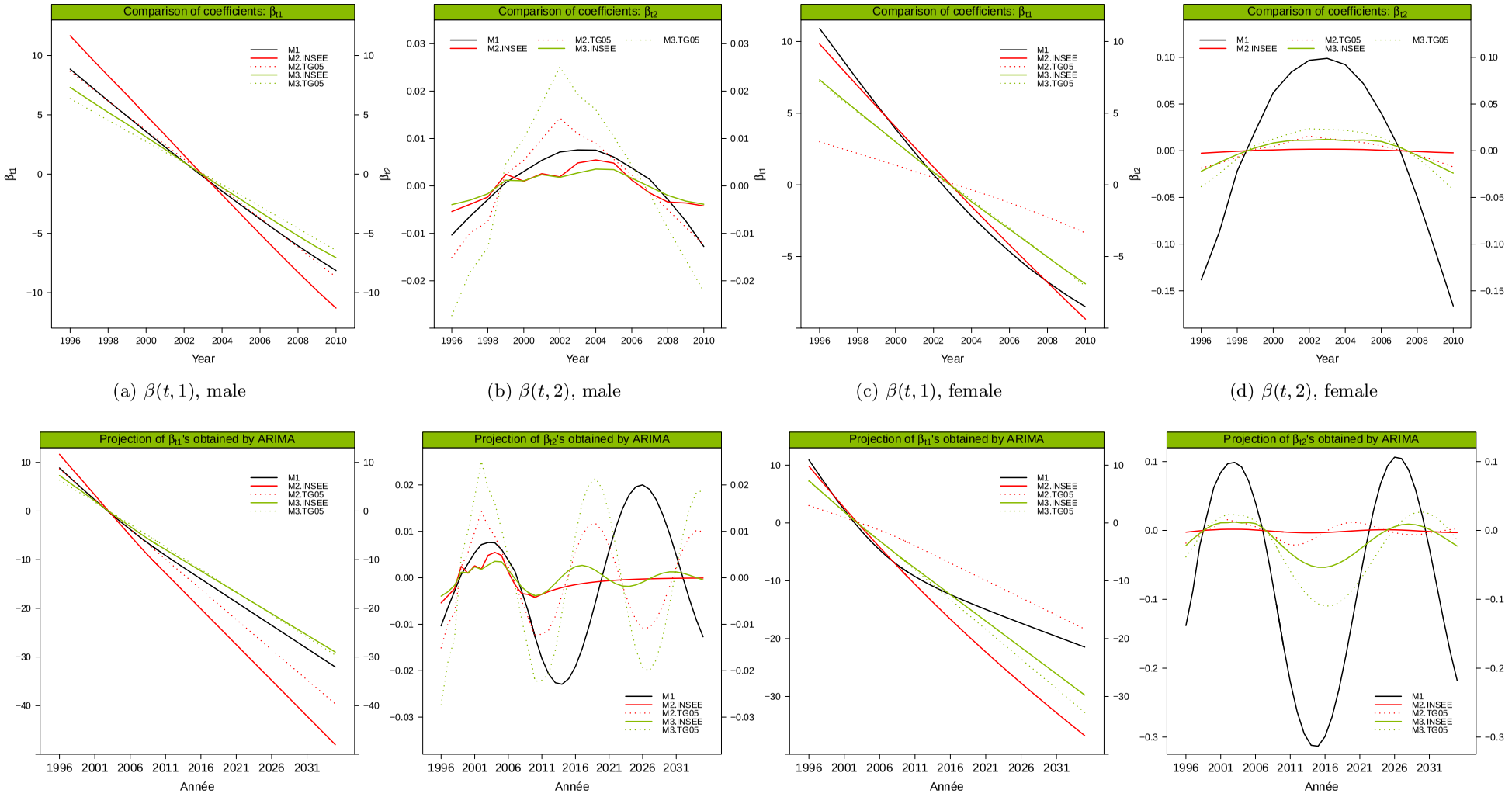

(a) $\beta(t,1)$, male (b) $\beta(t,2)$, male (c) $\beta(t,1)$, female (d) $\beta(t,2)$, female

(e) $\tilde{\beta}_{m,h,1}$, male (f) $\tilde{\beta}_{m,h,2}$, male (g) $\tilde{\beta}_{m,h,1}$, female (h) $\tilde{\beta}_{m,h,2}$, female

Figure 8: Estimated coefficients $\beta_{t,k}$ and projections for the models M1, M2 and M3 obtained by ARIMA with $K = 2$.

	Model & component		Model for the $\beta_{t,k}$	
Male population	M1	$k=1$	ARIMA(1,2,0)	$\beta_t = 2\,\beta_{t-1} - \beta_{t-2} + \mu + \phi(\beta_{t-1} - 2\,\beta_{t-2} + \beta_{t-3} - \mu) + Z_t$
		$k=2$	ARIMA(2,0,1) with zero mean	$\beta_t = \mu + \phi_1(\beta_{t-1} - \mu) + \phi_2(\beta_{t-2} - \mu) + Z_t + \theta\, Z_{t-1}$
	M2.INSEE	$k=1$	ARIMA(0,2,0)	$\beta_t = 2\,\beta_{t-1} - \beta_{t-2} + Z_t$
		$k=2$	ARIMA(1,0,0) with zero mean	$\beta_t = \mu\phi(\beta_{t-1} - \mu) + Z_t$
	M2.TG05	$k=1$	ARIMA(0,1,1)	$\beta_t = \beta_{t-1} + \mu + Z_t + \theta\, Z_{t-1}$
		$k=2$	ARIMA(4,0,0) with zero mean	$\beta_t = \mu + \phi_1(\beta_{t-1} - \mu) + \phi_2(\beta_{t-2} - \mu) + \phi_3(\beta_{t-3} - \mu) + \phi_4(\beta_{t-4} - \mu) + Z_t$
	M3.INSEE	$k=1$	ARIMA(0,2,0)	$\beta_t = 2\,\beta_{t-1} - \beta_{t-2} + Z_t$
		$k=2$	ARIMA(3,0,0) with zero mean	$\beta_t = \mu + \phi_1(\beta_{t-1} - \mu) + \phi_2(\beta_{t-2} - \mu) + \phi_3(\beta_{t-3} - \mu) + Z_t$
	M3.TG05	$k=1$	ARIMA(0,2,0)	$\beta_t = 2\,\beta_{t-1} - \beta_{t-2} + Z_t$
		$k=2$	ARIMA(4,0,0) with zero mean	$\beta_t = \mu + \phi_1(\beta_{t-1} - \mu) + \phi_2(\beta_{t-2} - \mu) + \phi_3(\beta_{t-3} - \mu) + \phi_4(\beta_{t-4} - \mu) + Z_t$
Female population	M1	$k=1$	ARIMA(1,2,0)	$\beta_t = 2\,\beta_{t-1} - \beta_{t-2} + \mu + \phi(\beta_{t-1} - 2\,\beta_{t-2} + \beta_{t-3} - \mu) + Z_t$
		$k=2$	ARIMA(2,0,1)	$\beta_t = \mu + \phi_1(\beta_{t-1} - \mu) + \phi_2(\beta_{t-2} - \mu) + Z_t + \theta\, Z_{t-1}$
	M2.INSEE	$k=1$	ARIMA(2,2,0)	$\beta_t = 2\,\beta_{t-1} - \beta_{t-2} + \mu + \phi_1(\beta_{t-1} - \mu) + \phi_2(\beta_{t-2} - \mu) + Z_t$
		$k=2$	ARIMA(3,0,0)	$\beta_t = \mu + \phi_1(\beta_{t-1} - \mu) + \phi_2(\beta_{t-2} - \mu) + \phi_3(\beta_{t-3} - \mu) + Z_t$
	M2.TG05	$k=1$	ARIMA(1,2,0)	$\beta_t = 2\,\beta_{t-1} - \beta_{t-2} + \mu + \phi(\beta_{t-1} - 2\,\beta_{t-2} + \beta_{t-3} - \mu) + Z_t$
		$k=2$	ARIMA(2,0,0) with zero mean	$\beta_t = \mu + \phi_1(\beta_{t-1} - \mu) + \phi_2(\beta_{t-2} - \mu) + Z_t$
	M3.INSEE	$k=1$	ARIMA(0,2,0)	$\beta_t = 2\,\beta_{t-1} - \beta_{t-2} + Z_t$
		$k=2$	ARIMA(2,0,0)	$\beta_t = \mu + \phi_1(\beta_{t-1} - \mu) + \phi_2(\beta_{t-2} - \mu) + Z_t$
	M3.TG05	$k=1$	ARIMA(0,2,0)	$\beta_t = 2\,\beta_{t-1} - \beta_{t-2} + Z_t$
		$k=2$	ARIMA(2,0,1)	$\beta_t = \mu + \phi_1(\beta_{t-1} - \mu) + \phi_2(\beta_{t-2} - \mu) + Z_t + \theta\, Z_{t-1}$

Table 9: Description of the models for the time-varying coefficients.

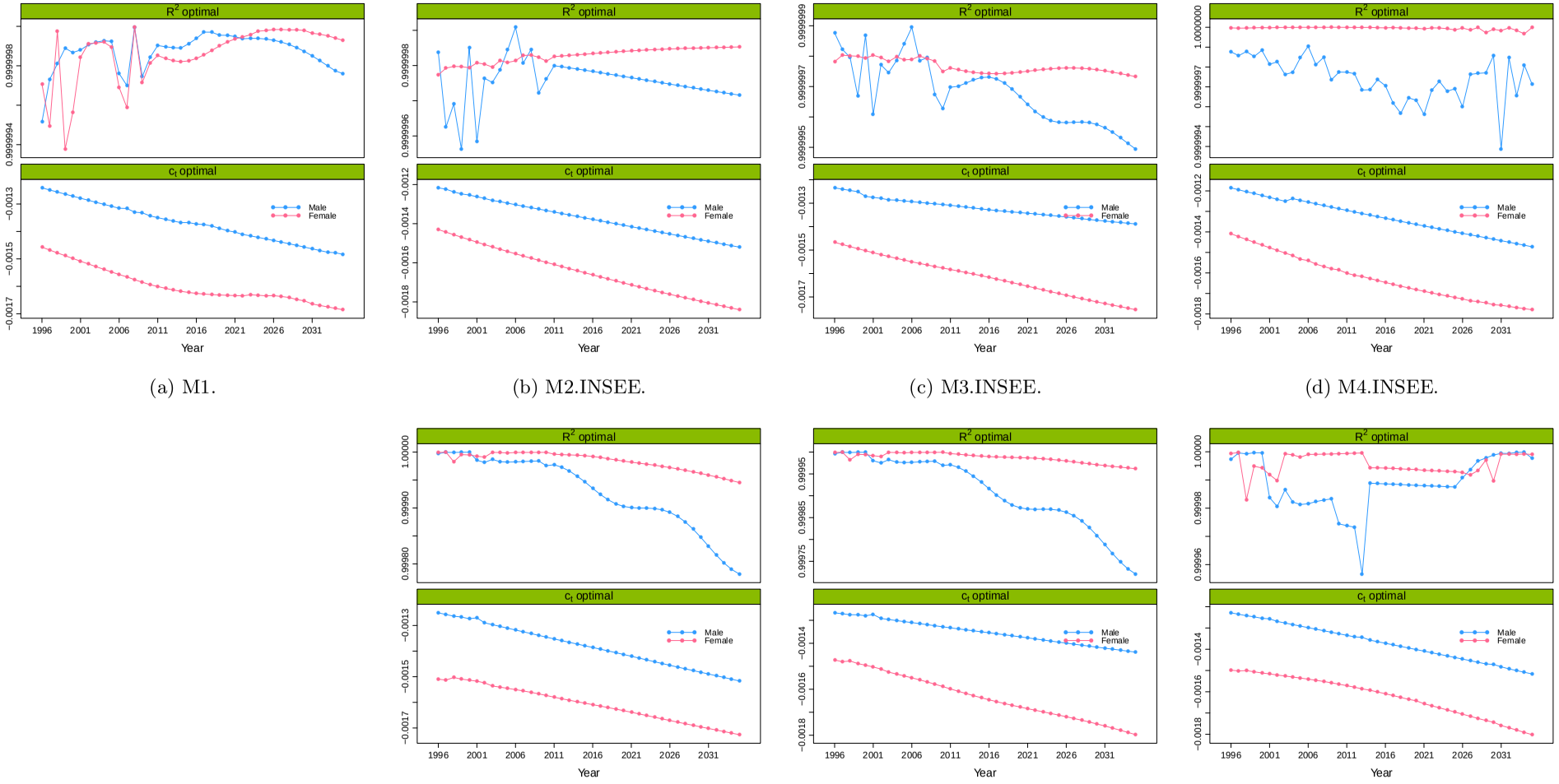

(a) M1. (b) M2.INSEE. (c) M3.INSEE. (d) M4.INSEE.

(e) M2.TG05. (f) M3.TG05. (g) M4.TG05.

Figure 9: R^2 et estimated c_t obtained by the completion method proposed by Denuit and Goderniaux (2005).

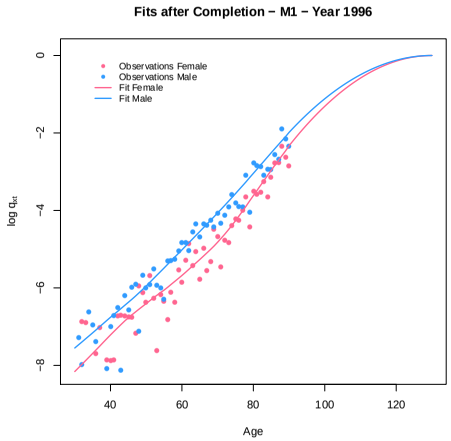

(a) M1.

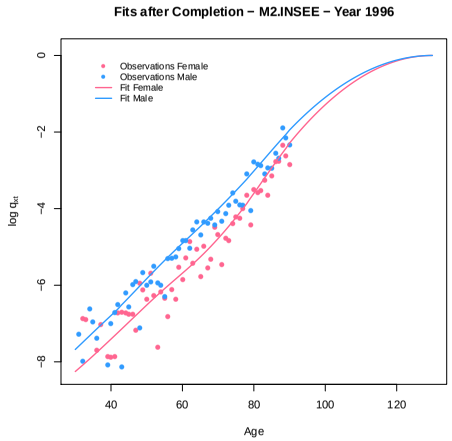

(b) M2.INSEE.

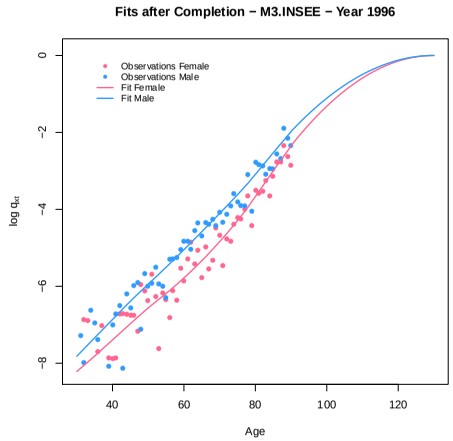

(c) M3.INSEE.

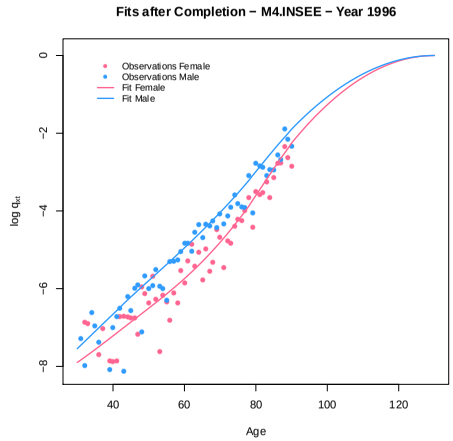

(d) M4.INSEE.

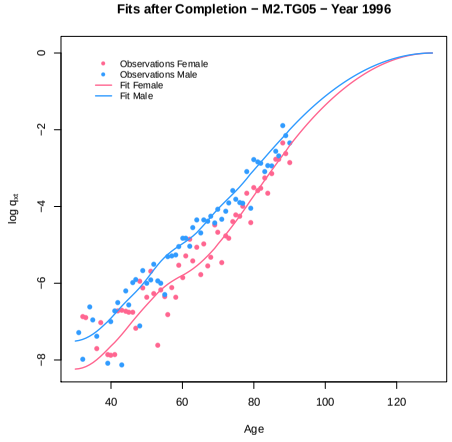

(e) M2.TG05.

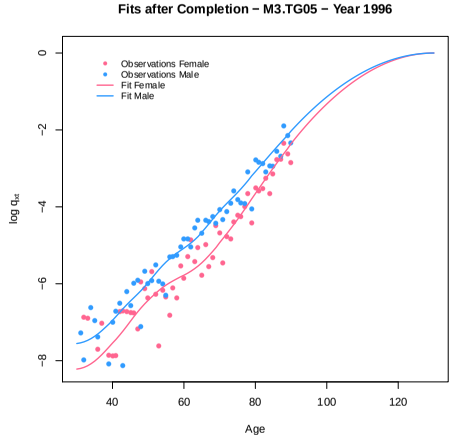

(f) M3.TG05.

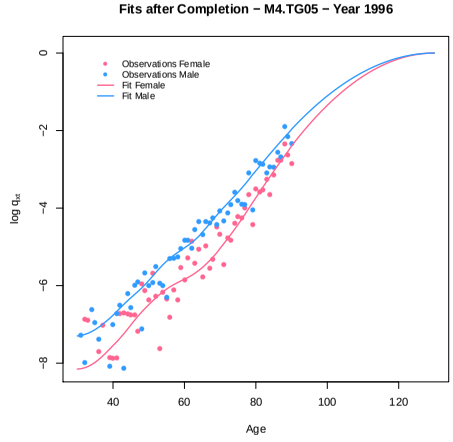

(g) M4.TG05.

Figure 10: Fits obtained after the completion for the calendar year 1996.

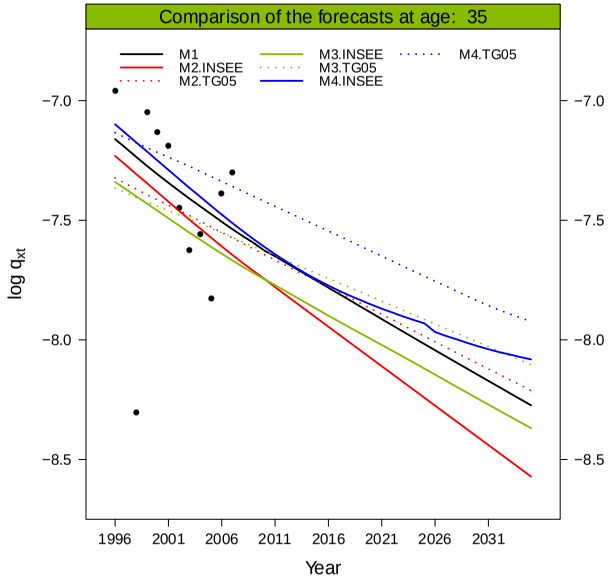

(a) Age 35, male.

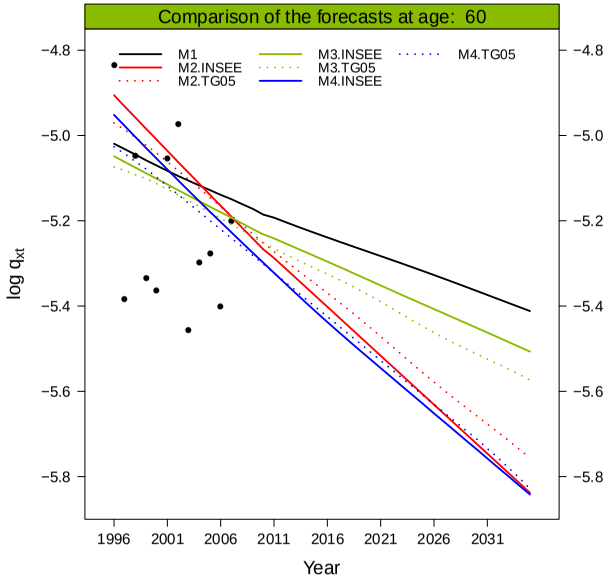

(b) Age 60, male.

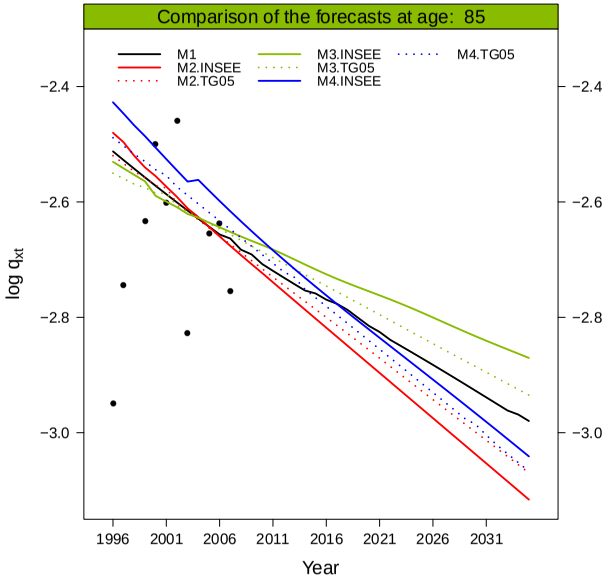

(c) Age 85, male.

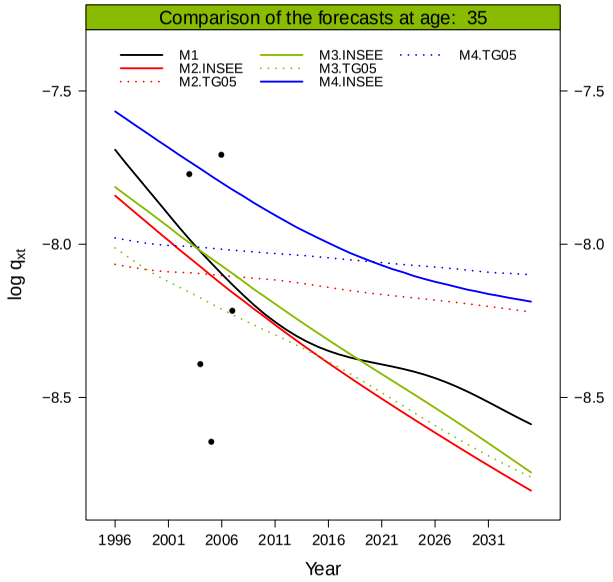

(d) Age 35, female.

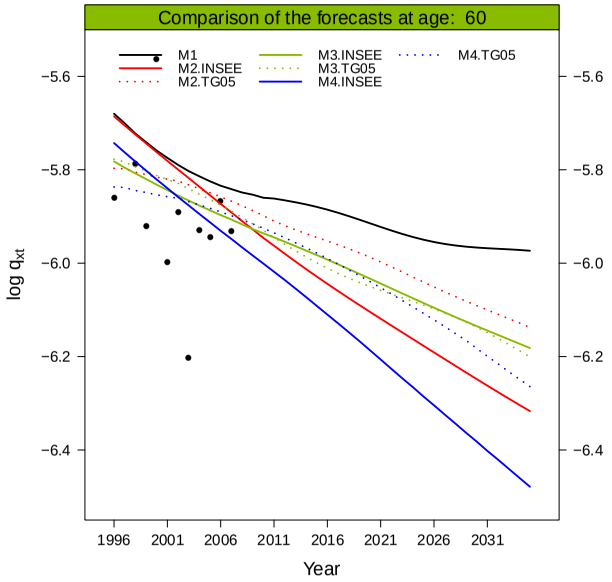

(e) Age 60, female.

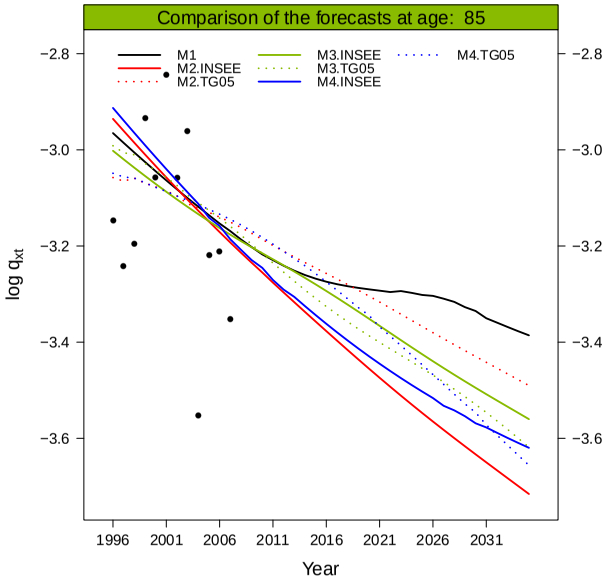

(f) Age 85, female.

Figure 11: Comparisons of the fits and forecasts for several attained ages, log scale.

		M1	M2.INSEE	M2.TG05	M3.INSEE	M3.TG05	M4.INSEE	M4.TG05
Male population	${}_{40}\overset{\nearrow}{e}_{30}$	38.75	38.91	38.88	38.77	38.81	38.83	38.80
	${}_{40}\overset{\nearrow}{e}_{40}$	36.97	37.33	37.22	37.04	37.11	37.25	37.23
	${}_{40}\overset{\nearrow}{e}_{50}$	32.85	33.44	33.18	32.93	33.00	33.40	33.32
	${}_{40}\overset{\nearrow}{e}_{60}$	25.24	25.66	25.59	25.14	25.35	25.57	25.66
	${}_{40}\overset{\nearrow}{e}_{70}$	16.56	16.61	16.65	16.46	16.54	16.41	16.58
	${}_{40}\overset{\nearrow}{e}_{80}$	9.26	9.17	9.28	9.25	9.30	8.87	9.14
	${}_{40}\overset{\nearrow}{e}_{90}$	4.31	4.20	4.33	4.26	4.38	4.03	4.23
	$\text{Med}\left[{}_{40}T_{50}\right]$	38.92	NA	NA	38.66	38.94	NA	NA
	$\text{Med}\left[{}_{40}T_{60}\right]$	28.25	28.94	28.72	28.21	28.37	28.76	28.73
	$\text{Med}\left[{}_{40}T_{70}\right]$	18.47	18.57	18.56	18.45	18.47	18.37	18.46
	$\text{Med}\left[{}_{40}T_{80}\right]$	10.29	10.19	10.30	10.35	10.36	9.88	10.13
	$\text{Med}\left[{}_{40}T_{90}\right]$	5.06	4.95	5.10	5.00	5.17	4.78	4.98
	$\text{H}\left[{}_{40}T_{30}\right]$	0.0008	0.0007	0.0007	0.0007	0.0007	0.0007	0.0007
	$\text{H}\left[{}_{40}T_{40}\right]$	0.0020	0.0017	0.0018	0.0019	0.0019	0.0018	0.0018
	$\text{H}\left[{}_{40}T_{50}\right]$	0.0060	0.0052	0.0055	0.0059	0.0058	0.0053	0.0054
	$\text{H}\left[{}_{40}T_{60}\right]$	0.0224	0.0209	0.0212	0.0235	0.0225	0.0216	0.0211
	$\text{H}\left[{}_{40}T_{70}\right]$	0.1003	0.0984	0.0979	0.1065	0.1028	0.1042	0.0995
	$\text{H}\left[{}_{40}T_{80}\right]$	0.4796	0.4827	0.4735	0.4999	0.4855	0.5199	0.4875
	$\text{H}\left[{}_{40}T_{90}\right]$	2.4047	2.4562	2.3781	2.4853	2.3891	2.6126	2.4523
Female population	${}_{40}\overset{\nearrow}{e}_{30}$	39.27	39.35	39.30	39.31	39.34	39.30	39.28
	${}_{40}\overset{\nearrow}{e}_{40}$	38.24	38.54	38.42	38.45	38.49	38.53	38.46
	${}_{40}\overset{\nearrow}{e}_{50}$	35.65	36.36	36.01	36.12	36.22	36.38	36.26
	${}_{40}\overset{\nearrow}{e}_{60}$	29.41	30.37	29.81	29.92	30.22	30.29	30.18
	${}_{40}\overset{\nearrow}{e}_{70}$	20.49	20.85	20.56	20.59	20.77	20.79	20.69
	${}_{40}\overset{\nearrow}{e}_{80}$	11.87	11.87	11.94	11.91	11.88	11.79	11.91
	${}_{40}\overset{\nearrow}{e}_{90}$	5.54	5.44	5.67	5.56	5.55	5.33	5.63
	$\text{Med}\left[{}_{40}T_{50}\right]$	NA	NA	NA	NA	NA	NA	NA
	$\text{Med}\left[{}_{40}T_{60}\right]$	32.85	34.21	33.24	33.48	33.81	33.99	33.66
	$\text{Med}\left[{}_{40}T_{70}\right]$	22.94	23.27	22.86	22.94	23.12	23.20	22.92
	$\text{Med}\left[{}_{40}T_{80}\right]$	13.31	13.28	13.40	13.37	13.29	13.17	13.35
	$\text{Med}\left[{}_{40}T_{90}\right]$	6.36	6.22	6.53	6.40	6.38	6.10	6.50
	$\text{H}\left[{}_{40}T_{30}\right]$	0.0004	0.0004	0.0004	0.0004	0.0004	0.0004	0.0004
	$\text{H}\left[{}_{40}T_{40}\right]$	0.0011	0.0009	0.0010	0.0010	0.0009	0.0009	0.0009
	$\text{H}\left[{}_{40}T_{50}\right]$	0.0031	0.0025	0.0027	0.0027	0.0026	0.0024	0.0025
	$\text{H}\left[{}_{40}T_{60}\right]$	0.0119	0.0098	0.0111	0.0108	0.0102	0.0101	0.0103
	$\text{H}\left[{}_{40}T_{70}\right]$	0.0573	0.0517	0.0563	0.0554	0.0534	0.0530	0.0547
	$\text{H}\left[{}_{40}T_{80}\right]$	0.3011	0.2883	0.2982	0.2966	0.2927	0.2953	0.2966
	$\text{H}\left[{}_{40}T_{90}\right]$	1.6871	1.6821	1.6509	1.6747	1.6630	1.7282	1.6563

Table 10: Single indices summarizing the lifetime probability distribution for cohorts of several ages in 1996 over 40 years.

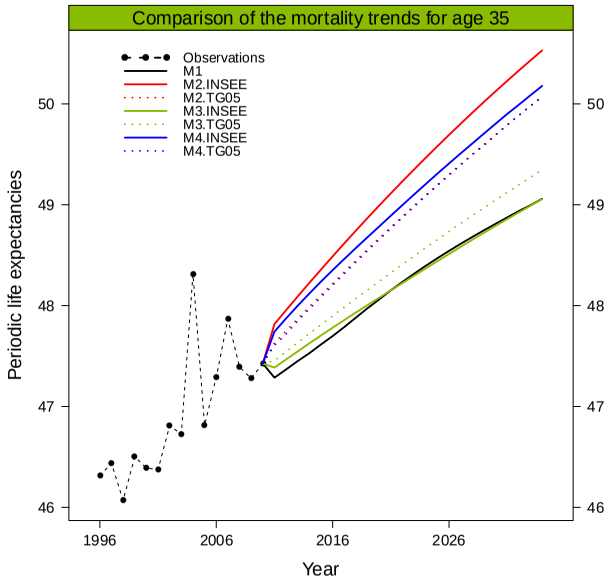

(a) Age 35, male.

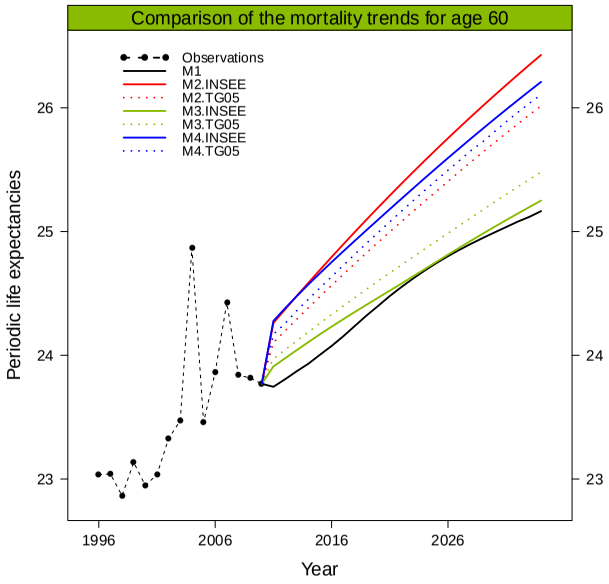

(b) Age 60, male.

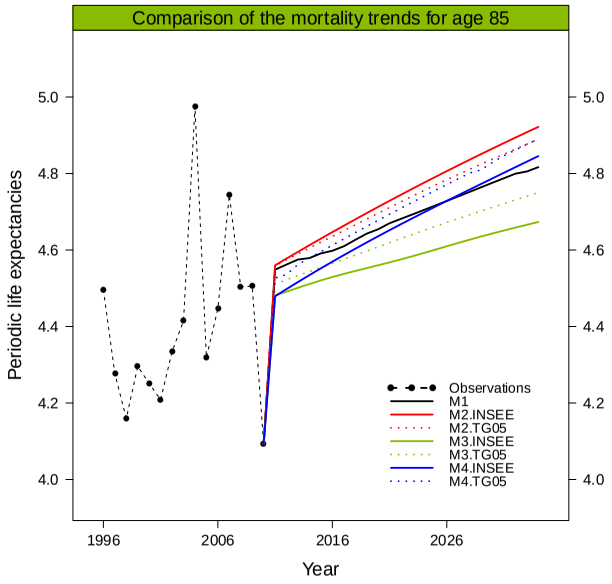

(c) Age 85, male.

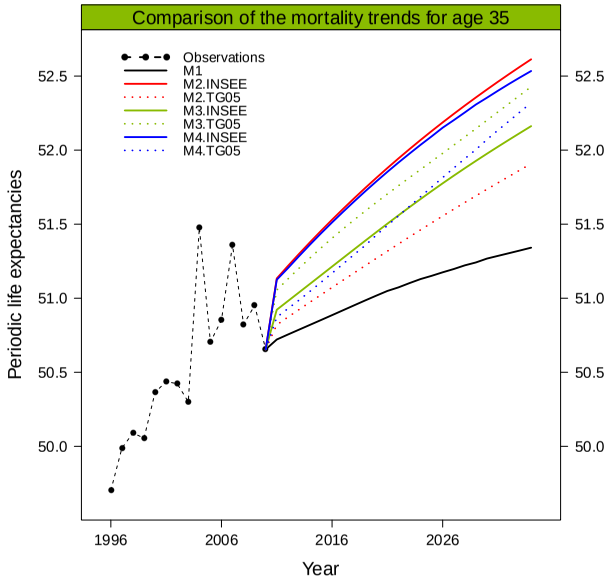

(d) Age 35, female.

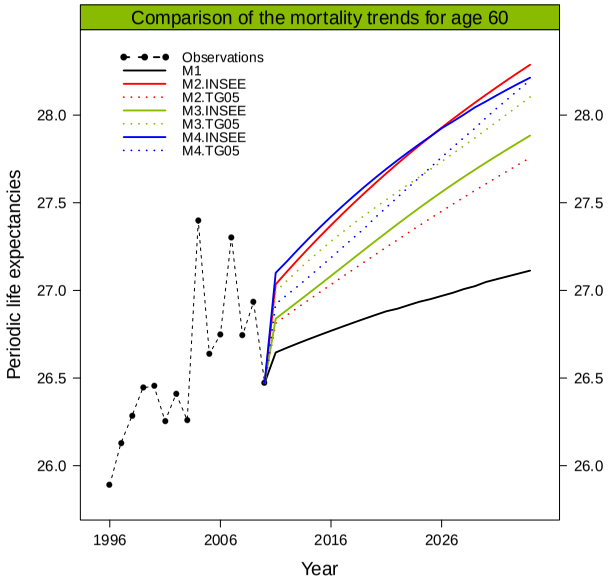

(e) Age 60, female.

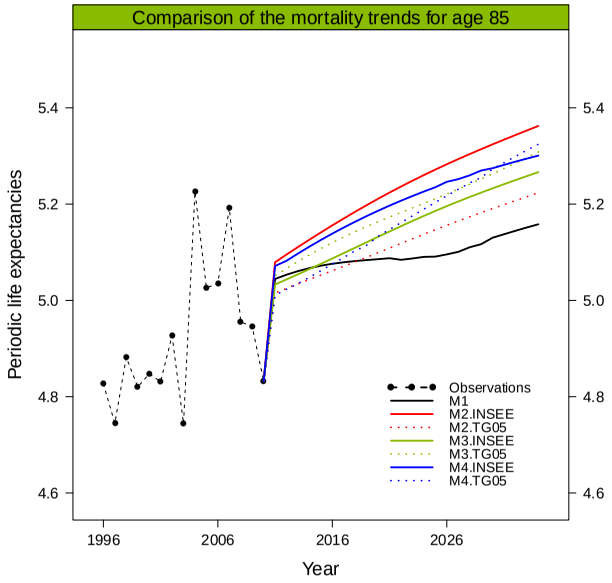

(f) Age 85, female.

Figure 12: Comparison of the trends in periodic life expectancies for several ages.

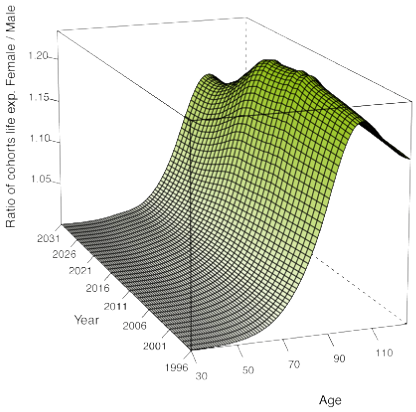

(a) M1.

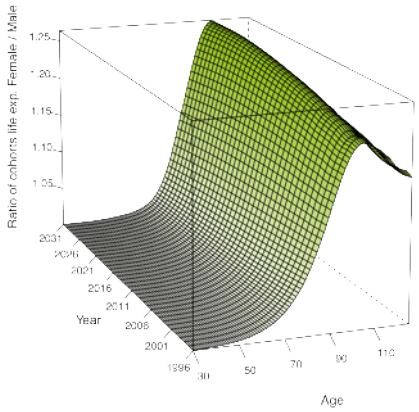

(b) M2.INSEE.

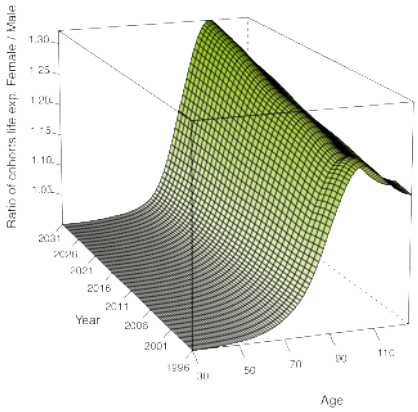

(c) M3.INSEE.

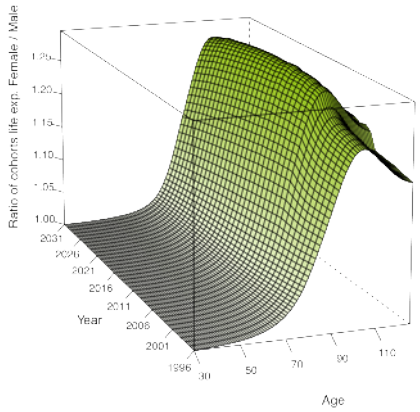

(d) M4.INSEE.

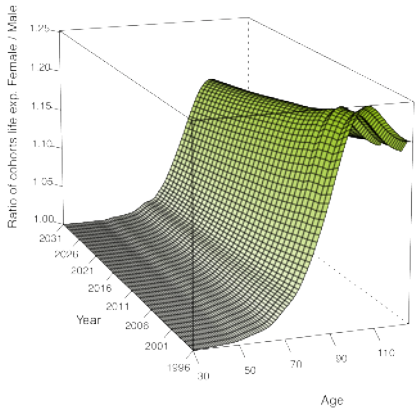

(e) M2.TG05.

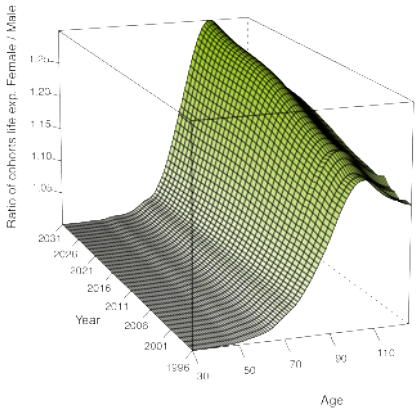

(f) M3.TG05.

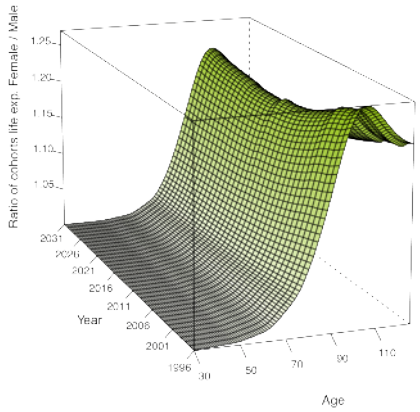

(g) M4.TG05.

Figure 13: Comparison of the male and female mortality, ratio of the cohort life expectancies over 5 years, female / male.

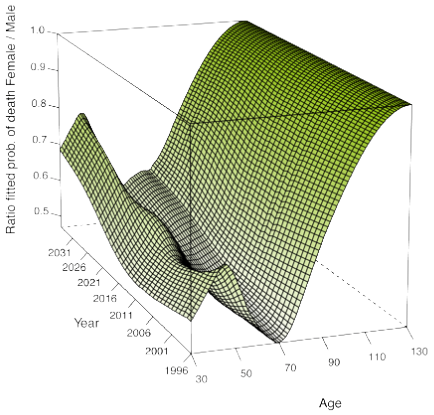

(a) M1.

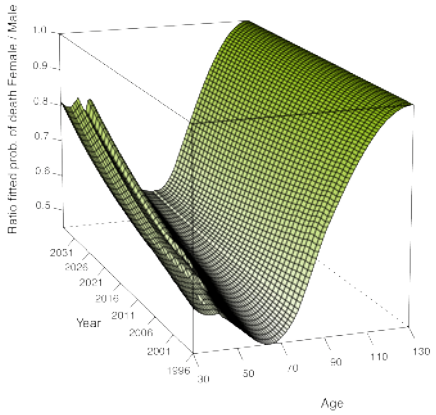

(b) M2.INSEE.

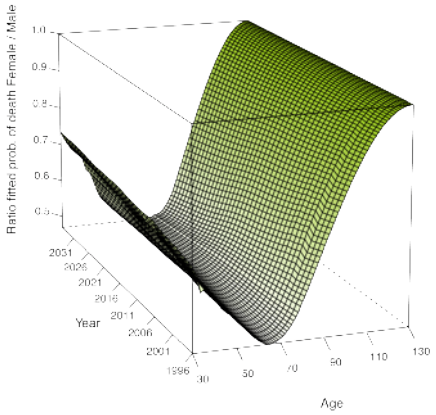

(c) M3.INSEE.

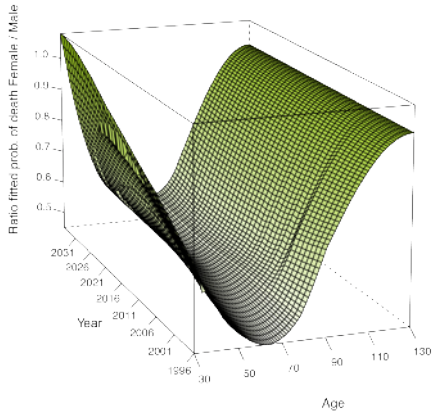

(d) M4.INSEE.

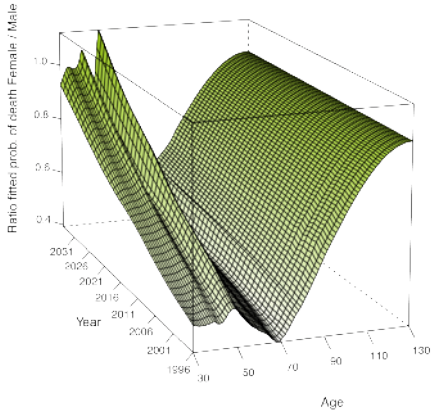

(e) M2.TG05.

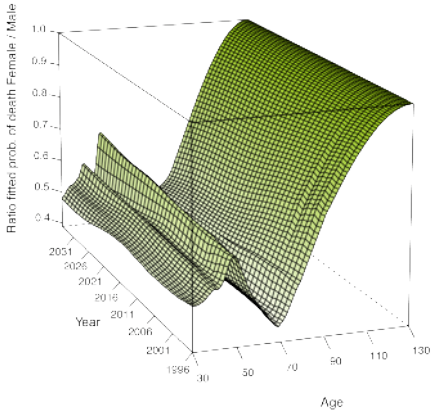

(f) M3.TG05.

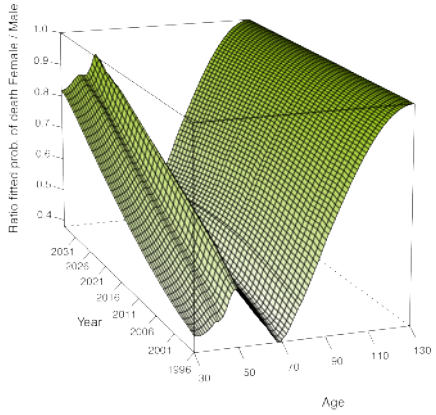

(g) M4.TG05.

Figure 14: Comparison of the male and female mortality, ratio of the fitted probabilities of death female / male.